Inorganic Chemistry

pubs.acs.org/IC

Forum Article

# Is Bismuth Really the "Green" Metal? Exploring the Antimicrobial Activity and Cytotoxicity of Organobismuth Thiolate Complexes

Liam J. Stephens,[†] Sarmishta Munuganti,[†] Rebekah N. Duffin, Melissa V. Werrett, and Philip C. Andrews*

Cite This: https://dx.doi.org/10.1021/acs.inorgchem.9b03550

Read Online

ACCESS | Metrics & More | Article Recommendations | Supporting Information



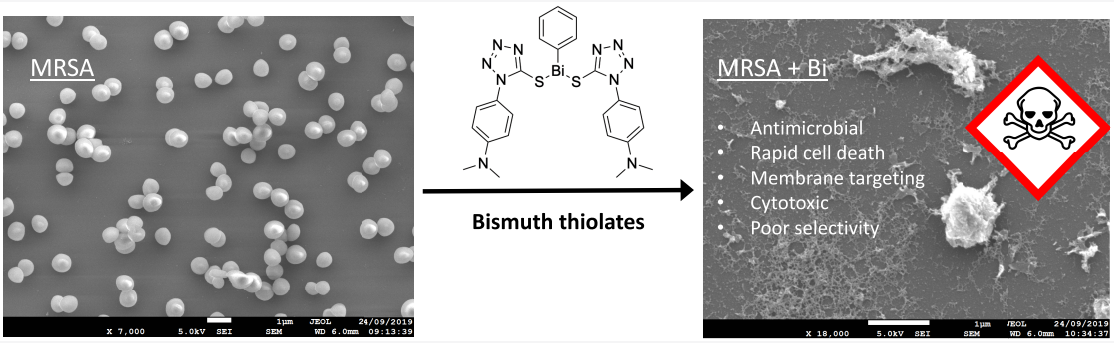


**ABSTRACT:** Antimicrobial resistance is becoming an ever-increasing threat for human health. Metal complexes and, in particular, those that incorporate bismuth offer an attractive alternative to the typically used organic compounds to which bacteria are often able to develop resistance determinants. Herein we report the synthesis, characterization, and biological evaluation of a series of homo- and heteroleptic bismuth(III) thiolates incorporating either one ($BiPh_2L$), two ($BiPhL_2$), or three ($BiL_3$) sulfur-containing azole ligands where LH = tetrazolethiols or triazolethiols (thiones). Despite bismuth typically being considered a nontoxic heavy metal, we demonstrate that the environment surrounding the metal center has a clear influence on the safety of bismuth-containing complexes. In particular, heteroleptic thiolate complexes ($BiPh_2L$ and $BiPhL_2$) display strong antibacterial activity yet are also nonselectively cytotoxic to mammalian cells. Interestingly, the homoleptic thiolate complexes ($BiL_3$) were shown to be completely inactive toward both bacterial and mammalian cells. Further biological analysis of the complexes revealed the first insights into the biological mode of action of these particular bismuth thiolates. Scanning electron microscopy images of methicillin-resistant *Staphylococcus aureus* (MRSA) cells have revealed that the cell membrane is the likely target site of action for bismuth thiolates against bacterial cells. This points toward a nonspecific mode of action that is likely to contribute to the poor selectivity's demonstrated by the bismuth thiolate complexes in vitro. Uptake studies suggest that reduced cellular uptake could explain the marked difference in activity between the homo- and heteroleptic complexes.

## INTRODUCTION

**Antimicrobial Resistance (AMR).** The potential impact that rapidly developing multiresistant bacteria could have on human health cannot be overstated. AMR is identified by the World Health Organization as one of the greatest threats we face globally, now and into the future.[1] Infections, which were once easily treated with a range of antibiotics, are now often resistant to our last line of defense compounds and in some cases have become fatal.[2,3] Despite efforts to discover new antibiotics, the rapid rates at which bacteria develop resistance is alarming. Novel antibiotics can become ineffective within months of market release, which can translate to a low return on investment to pharmaceutical companies. This challenging commercial model (coupled with the fact that antibiotic treatments are usually short-term) often means reduced antibiotic research and investment from large companies.[4] Metal and metal-based compounds have become increasingly investigated as novel antimicrobials because microbes often face difficulties in acquiring resistant determinants to these compounds. This contrasts to organic compounds, for which bacteria have already proven themselves to be adept at evolving mechanisms to break down or inactivate.[5]

**Metal Antimicrobials.** One of the more commonly known and widely used metals in antibacterial agents is silver. However, as the use of silver continues to expand, debates in

Special Issue: Bismuth - The Magic Element

Received: December 6, 2019

**Scheme 1. General Synthesis of Tetrazolethiols (a–f) and Triazolethiols (g–l) and the Corresponding Bismuth(III) Complexes 1a–1l, 2a–2f, and 3a–3l**

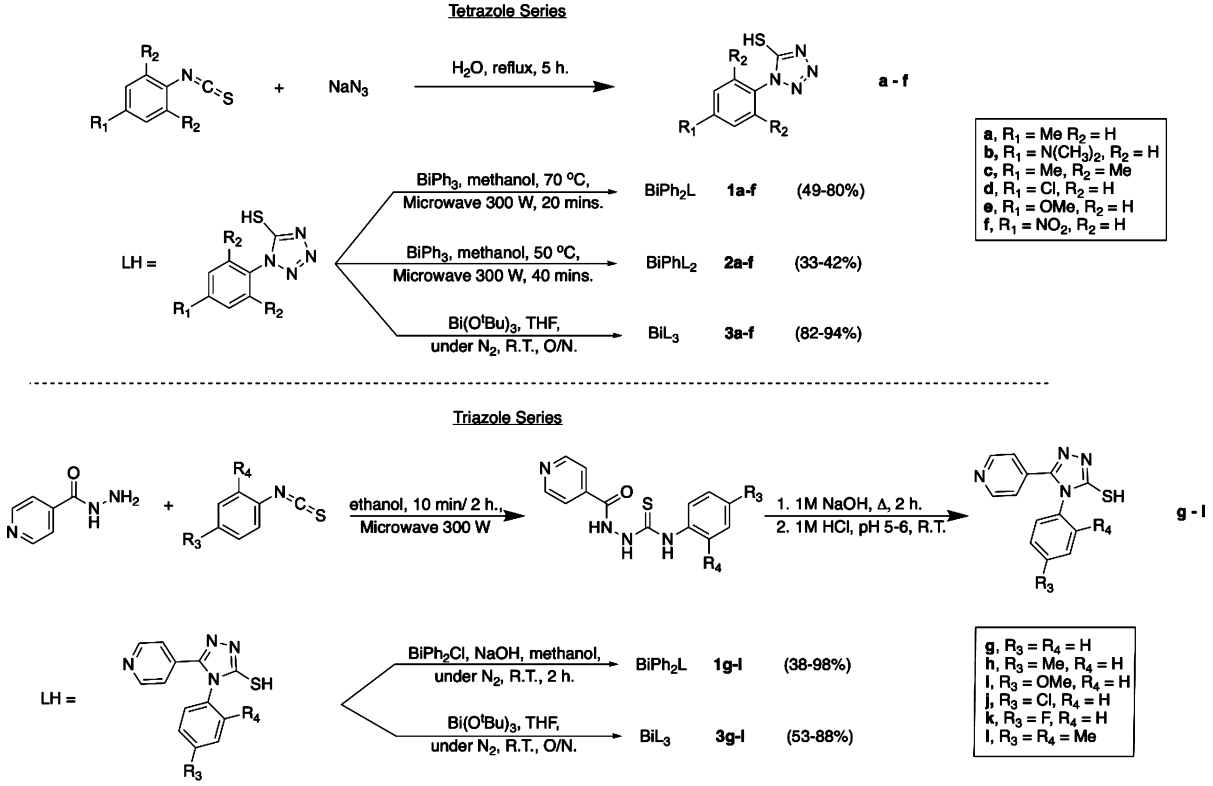


the literature have arisen that focus on major knowledge gaps relating to silver (nanoparticle) toxicity, environmental accumulation, and acquired bacterial resistance.[6,7] As such, we have turned our efforts toward investigating bismuth and its complexes as novel metal-based antimicrobial agents.

**Bismuth.** The lead-free movement has resulted in the replacement of lead with bismuth in a wide range of materials that encompass medicinal applications such as computed tomography contrast agents, to impart radiopacity, and a treatment for infections caused by the Gram-negative bacterium *Helicobacter pylori*. Most of these uses stem from the well-accepted nontoxicity of bismuth, which has been largely described as a surprisingly harmless element considering its position in the periodic table.[8] Bismuth compounds are most commonly known for their highly effective antimicrobial properties coupled with generally low human and environmental toxicity. As such, a number of bismuth compounds are used globally in combination therapies for the treatment of infections caused by *H. pylori* including bismuth subsalicylate (Pepto-Bismol) and colloidal bismuth subcitrate (CBS or De-Nol).[9,10]

A recent breakthrough by Sun and co-workers demonstrated that CBS and related bismuth(III) compounds can inhibit metallo-$\beta$-lactamases (MBLs), the enzymes responsible for deactivating the $\beta$-lactam class of antibiotics.[11] Inhibiting MBLs is potentially crucial in revitalizing the efficacy of $\beta$-lactam antibiotics, for which many are becoming obsolete because of AMR.

Despite the vast studies that have investigated the synthesis, characterization, and antimicrobial efficacy of *novel* bismuth complexes, there is still much to be explored regarding their structure–activity relationships and antimicrobial mode of action. Studies have demonstrated that the efficacy of organobismuth complexes against microbes is very dependent on the number and type of coordinating ligands.[12−16] Despite recent progress in this field, few studies have investigated the effects of these novel complexes toward human or human-like cells because bismuth is generally considered to be *nontoxic*.[8] This aspect is critical in understanding the selectivity of novel compounds for the target microbe, over "normal/healthy" cells. To elaborately state that new bismuth complexes will be nontoxic based on the known previous safe history of bismuth in medicine is often misconstrued. Metal toxicity is typically misunderstood and can be difficult to measure. It is important to understand that the toxicity of a metal is not constant and is affected by the surrounding ligands, oxidation state, solubility, particle size, and shape, as well as the environment that the metal/metal complex is exposed to.[17] Even for bismuth, it is known that all of the aforementioned factors can have a significant influence on their stability (e.g., pH-dependent ligand exchange and cluster formation), targeted activity, and toxicity.

There are a few studies that look at the toxic side effects of bismuth compounds, including but not limited to reduced cell viability from in vitro studies, to observations of neurotoxicity in humans. It has been reported that prolonged high level exposure to certain bismuth compounds can lead to altered neurofunction. Bismuth-induced neurotoxicity (or encephalopathy) is a rare side effect that has been reported in patients taking high and/or prolonged doses of bismuth subnitrate, subgallate, or subsalicylate.[18−20] However, generally withdrawal of the bismuth drug leads to complete recovery in short time periods.[20] An in vitro study from 2005 reports the reduced viability of testicular macrophages upon exposure to


https://dx.doi.org/10.1021/acs.inorgchem.9b03550
Inorg. Chem. XXXX, XXX, XXX−XXX

concentrations of bismuth citrate as low as 6.25 $\mu$M bismuth content.[21] These examples emphasize the importance of assessing the toxicity of novel bismuth compounds and how they can affect the viability of cells: we cannot assume they will be safe.

**Bismuth Heterocyclic Thiols.** N-Heterocyclic compounds play an important role in medicinal chemistry and are the active components in a range of drug molecules. Their medicinal properties include but are not limited to antiviral, antiinflammatory, analgesic, anticonvulsant, antiparasitic, antidiabetic, antihistaminic, antineuropathic, antihypertensive, as well as antifungal and antibacterial.[22,23] Resulting from the increased interest in these organic molecules and improved synthetic techniques, research has expanded into their use in bioinorganic chemistry, exploring the coordination of N-heterocyclic compounds to metals, with subsequent investigations into their medicinal properties. The motivation behind the inclusion of a sulfur moiety in these N-heterocyclic compounds is due to the thiophilic nature of bismuth and the hydrolytic and thermodynamic stability of bismuth thiolates. Despite this stability, Bi−S bonds are labile, which often translates to interesting interactions in biological systems with sulfur-containing proteins and peptides. While bismuth(III) thiolate complexes have been reported previously,[24,25] only a small number have been assessed for their antimicrobial activity.[12,13,26−28]

Herein we explore the synthesis, characterization, and biological evaluation of a series of tetrazole- and triazolethiols (thiones) and their corresponding bismuth(III) complexes. To probe for possible structure−activity trends, both homoleptic ($BiL_3$) and heteroleptic ($BiPh_2L$ and $BiPhL_2$) bismuth thiolates were targeted, where LH is either a series of substituted 1-(phenyl)-1*H*-tetrazole-5-thiols (thiones) or 1,2,4-triazole-3-thiols (thiones).

Free tetrazole- and triazolethiols (thiones) and their corresponding bismuth(III) complexes were tested against four clinically relevant strains of bacteria; methicillin-resistant *Staphylococcus aureus* (MRSA), vancomycin-resistant *Enterococcus faecalis* (VRE), *Escherichia coli* (*E. coli*), and *Pseudomonas aeruginosa* (*P. aeruginosa*). Furthermore, to probe their selectivity, the complexes were all assessed against cos-7 monkey kidney cells using the CellTiter-Blue viability assay and red blood cells using a hemolysis assay.

## RESULTS AND DISCUSSION

**Synthesis.** Tetrazolethiols (thiones) were synthesized based on previously published methods,[29] via the [3 + 2] cycloaddition of a substituted aryl isothiocyanate with sodium azide. After 5 h of heating at reflux in water, the desired compounds were acquired in good-to-moderate yields.

Triazolethiols (thiones) were synthesized in a two-step reaction process according to previously published methods.[30] First, a hydrazine carbothioamide derivative was formed following the reaction of an aryl isothiocyanate and isonicotinic hydrazide. Oxidative cyclization to the corresponding triazole was achieved after the addition of sodium hydroxide at reflux. The synthetic pathways for both the tetrazole- and triazolethiols and their corresponding yields (%) are outlined in Scheme 1 below.

The bismuth monotetrazolethiolate complexes **1a−1f** ($BiPh_2L$, where LH is a tetrazolethiol) were prepared by treating $BiPh_3$ with one of a series of substituted 1-(phenyl)-1*H*-tetrazole-5-thiols (**a−f**) in a 1.2:1 ratio under microwave conditions (300 W, 50 °C) in ethanol. After removal of the reaction vessel from the microwave, fine needles developed rapidly from the reaction solution and were filtered to give complexes **1a−1f**.

The formation of bismuth monotriazolethiolate complexes **1g−1l** ($BiPh_2L$, where L-Na is a sodium triazolethiolate synthesized in situ) was achieved following a salt metathesis reaction between $BiPh_2Cl$ and the sodium salts of triazolethiols **g−l**. The desired complexes precipitated from the reaction mixture and were isolated as pure solids after filtration and washing with cold water and acetone.

Bistetrazolethiolate complexes (**2a−2f**; $BiPhL_2$) were synthesized from the reaction of $BiPh_3$ with tetrazolethiols (**a−f**) in a 1:2.2 ratio. After 40 min of reaction under microwave conditions (300 W, 70 °C), the desired complexes were isolated as mixtures of *mono* (**1a−1f**) and *bis* complexes (**2a−2f**). Purification of the crude mixtures was achieved by trituration, recrystallization, and/or reverse-phase high-perfomance liquid chromatography (HPLC), which resulted in the isolation of compounds **2a−2f**. Unfortunately, bistriazole complexes could not be obtained as pure complexes because the aforementioned reaction conditions with triazolethiols **g−l** yielded a mixture of bismuth(III) mono- and bisthiolates that proved to be inseparable by a number of purification techniques. Attempts were made to control the formation of the bistriazoles by using solvent-free conditions, salt metathesis at reflux, and low temperatures (−75 and 0 °C), varying the reaction times and different solvent systems [tetrahydrofuran (THF), toluene, and hexane]. However, all of the aforementioned conditions resulted in the unsuccessful formation of the desired bistriazoles as single products. The mixtures that were isolated from the reaction solutions were unable to be separated via crystallization and a range of chromatography techniques (flash and HPLC) for the reason that the mono- and bistriazole species appeared to be in flux in solution. Given the lack of purity, these mixtures were not considered for use in biological studies.

Tristhiolato complexes (**3a−3l**; $BiL_3$, where LH is a tetrazole- or triazolethiol) were prepared following the overnight reaction of Bi(O$^t$Bu) with either tetrazolethiols (**a−f**) or triazolethiols (**g−l**) in a 1:3 ratio under Schlenk conditions. The synthetic pathways for all bismuth thiolates are outlined in Scheme 1.

**Characterization.** The compositions of all of the triazolethiols were confirmed by analytical methods such as $^1$H NMR, which matched the previously reported data.[30] The compositions of the tetrazolethiols were confirmed by $^1$H and $^{13}$C NMR, IR spectroscopy and electrospray ionization mass spectrometry (ESI-MS). The structures and compositions of the heteroleptic complexes **1a−1l** ($BiPh_2L$) and **2a−2f** ($BiPhL_2$) and the homoleptic complexes **3a−3l** ($BiL_3$) were also confirmed by $^1$H and $^{13}$C NMR, IR spectroscopy, ESI-MS, and elemental analysis (see the Experimental Section and Supporting Information for details). In general, the heteroleptic bismuth(III) thiolates displayed a downfield shift of the phenyl signals in both $^1$H and $^{13}$C NMR, consistent with previously published bismuth complexes.[13,15,28] For instance, in the case of complex **1c**, the phenyl protons are shifted to 8.27 (*o*), 7.57 (*m*), and 7.38 (*p*) ppm, all at lower frequencies relative to the analogous protons in $BiPh_3$ [$\delta$ = 7.76 (*o*), 7.38 (*m*), and 7.31 (*p*)]. The chemical shifts and integrals of the residual phenylbismuth and thiolate ligand signals in **1a−1l** and **2a−2f** also support the composition of bismuth(III)


https://dx.doi.org/10.1021/acs.inorgchem.9b03550
Inorg. Chem. XXXX, XXX, XXX−XXX

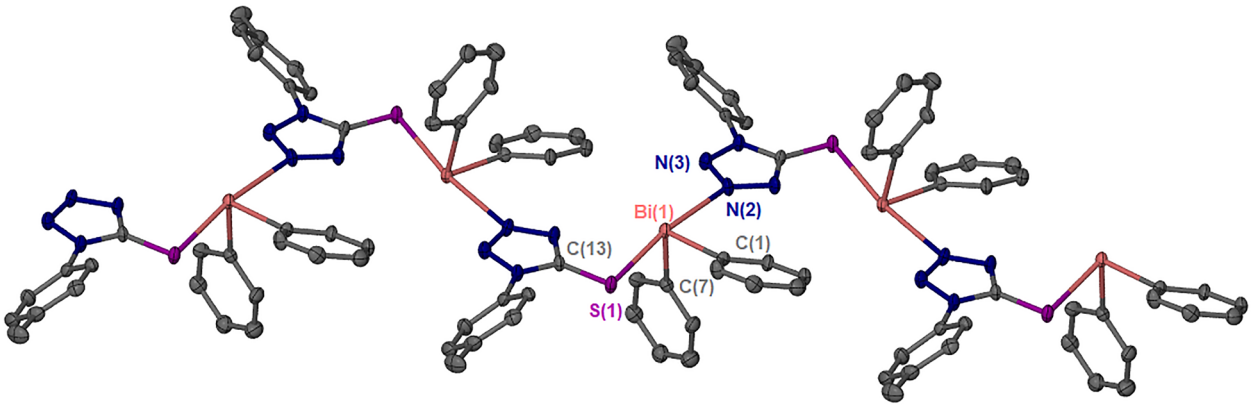


**Figure 1.** Extended polymeric structure of **1a** showing thermal ellipsoids at 50% probability. Hydrogen atoms have been omitted for clarity. Selected bond lengths (Å): Bi(1)−S(1), 2.647(2); Bi(1)−N(2), 2.779(7); Bi(1)−C(1), 2.243(8); Bi(1)−N(2), 2.779(7); Bi(1)−C(7), 2.237(8). Selected bond angles (deg): S(1)−Bi(1)−N(2), 171.07(16); C(1)−Bi(1)−S(1), 85.9(2); C(1)−Bi(1)−N(2), 90.0(3); C(7)−Bi(1)−S(1), 89.2(2).

complexes. For the homoleptic complexes **3a**−**3l** ($BiL_3$), the disappearance of the stretching frequency corresponding to S−H at approximately 2550−2600 $cm^{-1}$ suggests coordination to the bismuth metal center through the sulfur (thiolate forms of **a**−**l**). High-resolution mass spectrometry also confirmed formation of the homoleptic complexes **3a**−**3l**. A number of structures were also confirmed by single-crystal X-ray diffraction (XRD), which confirmed the data obtained from other analytical techniques (see below).

**X-ray Crystallography.** The crystals of 11 heteroleptic bismuth(III) thiolate complexes were obtained from the slow evaporation of either toluene, dimethyl sulfoxide (DMSO), or DMSO/toluene solutions of the isolated complexes. Using single-crystal XRD, the solid-state structures were elucidated. The asymmetric units observed for the monotetrazole and triazolethiolate complexes show structural similarities; however, they do not appear to be analogous. Between the mono- and bisbismuth(III) structures (complex series **1** and **2**, respectively), the bismuth(III) core adopts five- and six-coordinate environments. The environments vary from distorted tetrahedral, distorted disphenoidal/trigonal-bipyramidal, and square-pyramidal geometries, with all structures incorporating an empty void, presumed to be occupied by the stereochemically active lone pair (SALP). Variations in the geometry and coordination number of these structures appear to be influenced by the solvent system used for crystallization and can be observed in each structure.

Complexes **1a**, **1d**, **1f**, and **1g** all appear to be isostructural and crystallize as a weakly linked 1D polymer, with the bismuth(III) center adopting a six-coordinate, distorted octahedral geometry (Figure 1). The length of the bismuth core interaction for each complex is within the sum of the van der Waals radii of bismuth and nitrogen, and the Bi−S bond distances listed are typical of bismuth(III) arylthiolate complexes.[13,28,31,32] These structural motifs have been observed within previously synthesized bissulfonate complexes.[33] Similar polymeric chain-like structures have been observed where the four-coordinate bismuth(III) atoms are bridged between a dative nitrogen interaction from either an adjacent triazole or tetrazole group or pyridyl nitrogen. The structures present near-linear S−Bi−N bond angles with an average value of 170.6°.

Complexes **1h**, **1k**, and **1l** obtained from mixtures of DMSO and toluene all adopt distorted disphenoidal motifs (Figure 2).

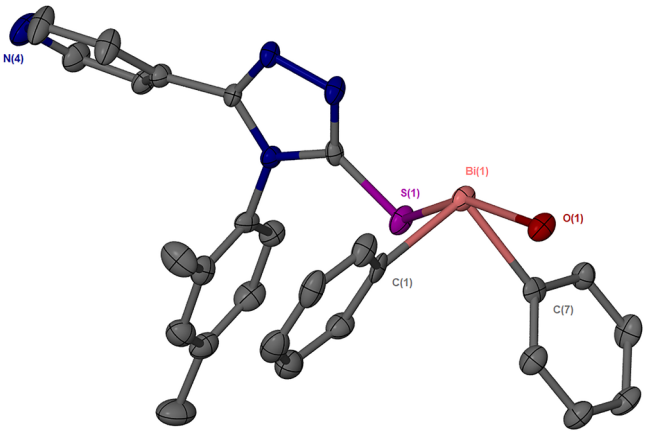


**Figure 2.** Molecular structure of **1l** showing thermal ellipsoids at 50% probability. Hydrogen atoms have been omitted for clarity. Selected bond lengths (Å): Bi(1)−C(1), 2.263(6); Bi(1)−C(7), 2.238(6); Bi(1)−O(1), 2.616(4); Bi(1)−S(1), 2.6601(13). Selected bond angles (deg): S(1)−Bi(1)−O(1), 158.39(9); C(7)−Bi(1)−C(1), 97.6(2); S(1)−Bi(1)−C(1), 92.83(14).

The spatial arrangement of this homometallic monomer unit is similar to previously synthesized heteroleptic sulfonate complexes.[33] The planes formed by the S−Bi−O and C−Bi−C interactions display angles of 158.1(5) and 99.0(11)°, leaving a large void across the S−Bi−O bond and trans to the two phenyl groups. Again, this void is expected to be occupied by the SALP.[31]

Analysis of the bis structures **2b** and **2d** shows the bismuth core adopting a five-coordinate geometry, where the fifth interaction can be attributed to a tetrazolato nitrogen. In the example **2d**, the overall geometry of the structure is a dimerized distorted square-based pyramid as a result of the covalent Bi−O and Bi−S bonds and two dative interactions (Figure 3). The involvement of the SALP from the bismuth core forming two dative interactions with one DMSO and a nitrogen atom from a neighboring tetrazolethiolate can be observed, with bond lengths of 2.447(4) and 2.700(4) Å. The O−Bi−S and S−Bi−N angles both sit at 167.64(10) and 167.61(10)°; these angles are consistent with previously reported bismuth thiolate structures.[13]

**Antibacterial Studies.** *Disk Diffusion and Minimum Inhibition Concentrations (MICs).* All of the parent tetrazole-


https://dx.doi.org/10.1021/acs.inorgchem.9b03550
Inorg. Chem. XXXX, XXX, XXX−XXX

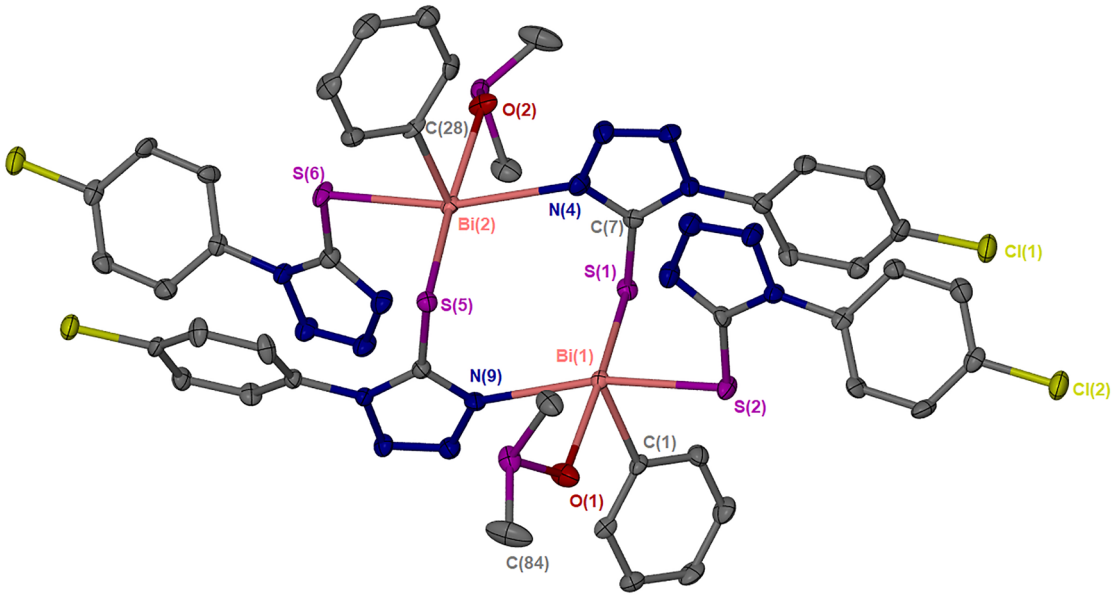


**Figure 3.** Molecular structure of **2d** showing thermal ellipsoids at 50% probability. Hydrogen atoms have been omitted for clarity. Selected bond lengths (Å): Bi(1)−S(7), 2.6859(13); Bi(1)−S(3), 2.7421(14); Bi(1)−N(30), 2.706(4); Bi(1)−C(33), 2.248(5); Bi(1)−O(4), 2.444(4); Bi(3)−S(11), 2.7475(14); Bi(3)−S(1), 2.6876(13); Bi(3)−N(46), 2.700(4); Bi(3)−O(9), 2.447(4); Bi(3)−C(2), 2.252(5). Selected bond angles (deg): S(7)−Bi(1)−N(30), 167.61(10); O(4)−Bi(1)−S(3), 168.18(9); C(33)−Bi(1)−S(7), 82.60(13); C(33)−Bi(1)−N(30), 87.13(16); N(30)−Bi(1)−S(3), 88.77(10). One of two complex moieties of the asymmetric unit is shown. Disorder of the secondary residual DMSO solvent molecule has been modeled over two positions and omitted for clarity (Figure S1).

and triazolethiols and their corresponding bismuth(III) complexes were screened against four clinically relevant strains of bacteria: two Gram-positive (MRSA and VRE) and two Gram-negative (*E. coli* and *P. aeruginosa*). The preliminary activity of the complexes against the bacteria was assessed using a Kirby−Bauer disk diffusion assay, at a set concentration of 400 $\mu$g/mL.

Disk diffusion assays revealed that only the bismuth(III) monothiolate (**1a−1l**; $BiPh_2L$) and bisthiolate (**2a−2f**; $BiPhL_2$) complexes inhibited the growth of bacteria at 400 $\mu$g/mL, with clear zones of inhibition observed for all of these particular complexes against all four strains of bacteria. The parent tetrazole- and triazolethiols (thiones), as well as the bismuth(III) tristhiolate complexes (**3a−3l**; $BiL_3$), did not show any antibacterial activity, with a confluent lawn of bacteria observed against all strains of bacteria. This marked difference in activity between homo- and heteroleptic bismuth(III) complexes has been observed previously.[13,16]

The in vitro activity of the active heteroleptic complexes **1a−1l** and **2a−2f** was next evaluated by calculating the MIC against the aforementioned strains of bacteria using a broth microdilution method (see the Experimental Section for details). The MIC results demonstrated the significant antibiotic activity of all of the heteroleptic (mono and bis) bismuth(III) complexes from both classes of azole compounds, against all four bacterial strains tested (Table 1). The complexes (**1a−1l** and **2a−2f**) proved to be a highly active species, with MIC values ranging from 0.39 to 21.50 $\mu$M (0.67−25 $\mu$g/mL; Table 1). In general, higher activities were seen for the tetrazole-containing complexes (**1a−1f** and **2a−2f**) relative to the triazole complexes (**1g−1l**). In order to confirm the lack of activity of the homoleptic bismuth complexes **3a−3l** (as shown in disk diffusion assays), MIC assays were conducted for these compounds against the four strains of bacteria. Unsurprisingly, all homoleptic complexes (**3a−3l**) showed no activity at the highest concentration tested (400 $\mu$g/mL).

**Table 1. Antibacterial Activities of Complexes 1a−1l, 2a−2f, and $BiPh_3$ against MRSA, VRE, *E. coli*, and *P. aeruginosa*[a]**

| | $\mu$M ($\mu$g/mL) | | | |
|---|---|---|---|---|
| | MRSA | VRE | *E. coli* | *P. aeruginosa* |
| **1a** | 2.82 (1.56) | 5.63 (3.13) | 1.41 (0.78) | 2.82 (1.56) |
| **1b** | 2.68 (1.56) | 5.36 (3.13) | 1.34 (0.78) | 2.68 (1.56) |
| **1c** | 2.68 (1.56) | 5.36 (3.13) | 0.67 (0.39) | 2.68 (1.56) |
| **1d** | 2.72 (1.56) | 5.44 (3.13) | 0.68 (0.39) | 2.72 (1.56) |
| **1e** | 2.74 (1.56) | 2.74 (1.56) | 1.37 (0.78) | 2.74 (1.56) |
| **1f** | 5.33 (3.13) | 2.67 (1.56) | 2.67 (1.56) | 5.33 (3.13) |
| **2a** | 4.67 (3.13) | 2.33 (1.56) | 2.33 (1.56) | 4.67 (3.13) |
| **2b** | 4.30 (3.13) | 2.15 (1.56) | 2.15 (1.56) | 4.30 (3.13) |
| **2c** | 4.30 (3.13) | 2.15 (1.56) | 2.15 (1.56) | 4.30 (3.13) |
| **2d** | 4.41 (3.13) | 2.20 (1.56) | 2.20 (1.56) | 4.41 (3.13) |
| **2e** | 4.46 (3.13) | 2.23 (1.56) | 2.23(1.56) | 4.46 (3.13) |
| **2f** | 4.27 (3.13) | 2.14 (1.56) | 2.14 (1.56) | 4.27 (3.13) |
| **1g** | 12.5 (9.90) | 3.13 (2.47) | 12.5 (9.90) | 25 (19.80) |
| **1h** | 12.5 (10.25) | 3.13 (2.56) | 12.5 (10.25) | 25 (20.50) |
| **1i** | 12.5 (10.65) | 6.25 (5.33) | 12.5 (10.65) | 25 (21.30) |
| **1j** | 12.5 (21.50) | 12.5 (10.75) | 12.5 (21.50) | 25 (21.50) |
| **1k** | 12.5 (10.35) | 6.25 (5.18) | 12.5 (10.35) | 25 (10.35) |
| **1l** | 12.5 (10.60) | 6.25 (5.30) | 6.25 (5.30) | 25 (21.20) |
| $BiPh_3$ | 28.40 (12.5) | 14.20 (6.25) | (>50) | (>50) |

[a]The MICs of complexes **3a−3f** were not included in the table because these complexes were shown to possess no antibacterial activities at 400 $\mu$g/mL in disk diffusion assays.

Interestingly, for the tetrazole complexes (**1a−1f** and **2a−2f**), the lowest MICs were observed against the Gram-negative strain, *E. coli*. This result was surprising because it has been previously shown that bismuth(III) complexes tend to inhibit Gram-positive bacteria at much lower concentrations[13,28,34] (as


https://dx.doi.org/10.1021/acs.inorgchem.9b03550
Inorg. Chem. XXXX, XXX, XXX−XXX

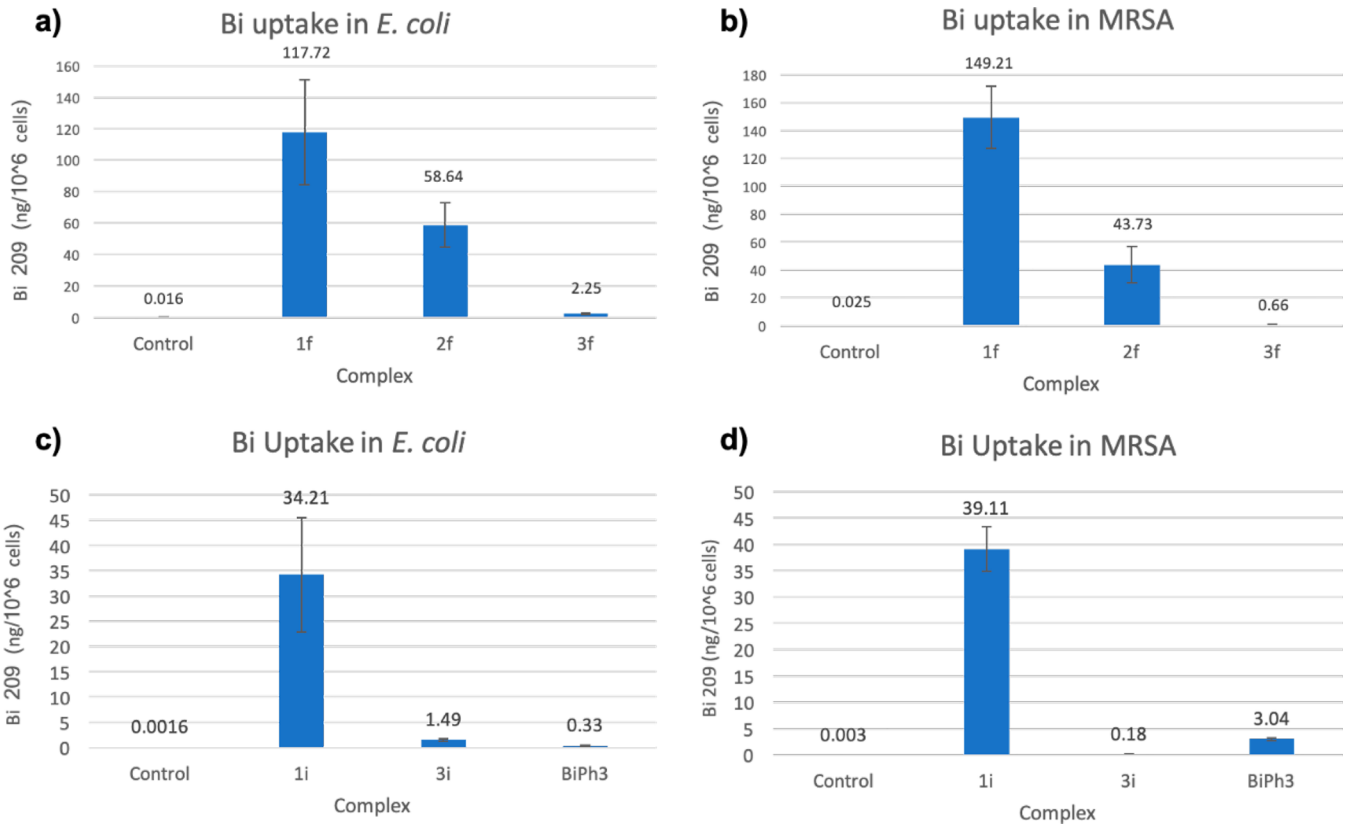


**Figure 4.** Cellular uptake of bismuth(III) tetrazolethiolate complexes **1f**, **2f**, and **3f** (a and b) and bismuth(III) triazolethiolate complexes **1i**, **3i**, and $BiPh_3$ (c and d), as measured by ICP-MS.

was the case with triazole complexes **1g**−**1l**), believed to be a result of the inability of such compounds to cross the additional outer membrane present in Gram-negative bacteria.[35] The potent activity of the tetrazole compounds (**1a**−**1f** and **2a**−**2f**) relative to the triazole complexes (**1g**−**1l**) against the Gram-negative pathogens *E. coli* and *P. aeruginosa* is not a consequence of their respective lipophilicities. *C* log *P* values (predicted using *ChemDraw 18.1*; Table S2) suggest that there is no significant difference in their projected lipophilicities that may have contributed to one set of complexes being more active than the other against these particular strains of Gram-negative bacteria.

The small range of MICs observed across the spectrum of complexes suggests that subtle changes in the thiolate ligand have little impact on the antibacterial activity. For instance, against MRSA, both the active tetrazole- (**1a**−**1f** and **2a**−**2f**) and triazole-containing complexes (**1g**−**1l**) have only a 2-fold difference in their MICs between the most active complexes in their series (e.g., 12.5 $\mu$M: **1g**−**1h** and **1k**−**1l**) and the least active complex (e.g., 25 $\mu$M: **1j**).

Despite there being a clear difference in the activity between the homo- and heteroleptic bismuth thiolate complexes, the MIC results demonstrated that the degree of thiolate substitution (i.e., mono- vs bisthiolate) also has little impact on the biological activity of the complexes. When the MICs of the mono complexes **1a**−**1f** ($BiPh_2L$) are compared with the analogous bis complexes **2a**−**2f** ($BiPhL_2$), there are no substantial differences in their respective MICs against all four strains of bacteria (Table 1).

**Bacterial Cell Uptake.** To investigate the differences in the antibacterial activity between the homoleptic bismuth thiolates and the heteroleptic analogues, the cellular uptake of $Bi^{209}$ in MRSA and *E. coli* was evaluated and quantified using inductively coupled plasma mass spectrometry (ICP-MS). The assay was conducted in order to further understand whether the increased biological activity of the heteroleptic bismuth(III) complexes could be a direct result of an increase in the cellular uptake of these particular complexes relative to their homoleptic counterparts. Since previous studies had indicated that, within each class of compound, there was little difference in the antimicrobial activity (Table 1), only one ligand for each class (tetrazole and triazole) was chosen for this study (**f** and **i**). A control, with no bismuth complex added, and $BiPh_3$ were included in this study. In order to directly compare the uptake of different complexes at the same concentration, complex concentrations of 5.3 $\mu$M (for complexes **1f**, **2f**, and **3f**) and 12.5 $\mu$M (for complexes **1i**, **3i**, and $BiPh_3$) were added to MRSA and *E. coli* bacteria.

After the complexes were exposed to bacterial cells for 24 h, the cells were first washed and digested, before $Bi^{209}$ content was analyzed via ICP-MS (see the Experimental Section for details of the procedure). The results obtained from ICP-MS revealed that there is a significant increase in the cellular uptake of $Bi^{209}$ for the most biologically active (heteroleptic) complexes (as shown by MICs), **1f**, **1i**, and **2f**, relative to their homoleptic bismuth(III) tristhiolate counterparts, **3f** and **3i**, as well as $BiPh_3$. This trend is clearly evident from the uptake graphs shown in Figure 4. The values obtained were also consistent between bacterial strains (MRSA and *E. coli*), with the $Bi^{209}$ uptake significantly lower for homoleptic bismuth(III) complexes (**3f** and **3i**), further suggesting a direct correlation between the complex cell uptake and biological


https://dx.doi.org/10.1021/acs.inorgchem.9b03550
Inorg. Chem. XXXX, XXX, XXX−XXX

activity. It is clearly evident that complexes of the type $BiPh_2L$ have the greatest uptake in bacterial cells, followed by the bis complexes ($BiPhL_2$), with the tristetrazole/triazole complexes ($BiL_3$) the lowest (mono > bis > tris). This reinforces the observation that higher uptake is correlated with higher antibacterial activity and that the activity is clearly linked to the lepticity of the complex. In general, it can be concluded from this assay that there is a direct correlation between the antibacterial activity and complex cellular uptake, with the most active complexes giving the largest readings of $Bi^{209}/10^6$ bacterial cells.

**Time-Kill Assays.** Continuing to probe the mode of action (bacteriostatic vs bactericidal) for the bismuth thiolates, we performed time-kill assays on example complexes **1b** and **2b** using MRSA and *E. coli*. Aliquots of brain heart infusion (BHI) broth containing overnight cultured bacteria with various concentrations of complexes **1b** and **2b** were serially diluted in phosphate-buffered solution (PBS) and plated on freshly prepared nutrient agar or Luria−Bertani (LB) plates at 0, 1, 3, 6, and 24 h. Incubation of the inoculated plates at 37 °C for 24 h revealed the bacterial survivors as colony-forming units (CFU) per milliliter.

Colony counting of bacterial survivors revealed the concentration-dependent killing profiles of complexes **1b** and **2b**, with the antimicrobial action observed as being bacteriostatic at MIC and MIC × 2 concentrations (Figure 5). The number of viable cells remained consistent with the starting inoculum (approximately $5 \times 10^5$ CFU/mL) at MIC and MIC × 2 concentrations at all time points analyzed in the 24 h assay. However, at MIC × 4 concentrations, complexes **1b** and **2b** both displayed rapid bactericidal activity against both strains of bacteria (Figure 5). After just 1 h, no viable cells were observed when *E. coli* was exposed to complexes **1b** and **2b** at MIC × 4 concentrations. For MRSA, slower killing kinetics were shown as no viable cells were observed at the 6 h time point for complex **1b**, while no viable cells were present after 24 h of exposure of cells to complex **2b**. It is, however, important to note that no time points were analyzed between 6 and 24 h, and it is likely that complex **2b** (at MIC × 4) is sufficient enough to completely eradicate all remaining bacterial survivors within these two particular time frames.

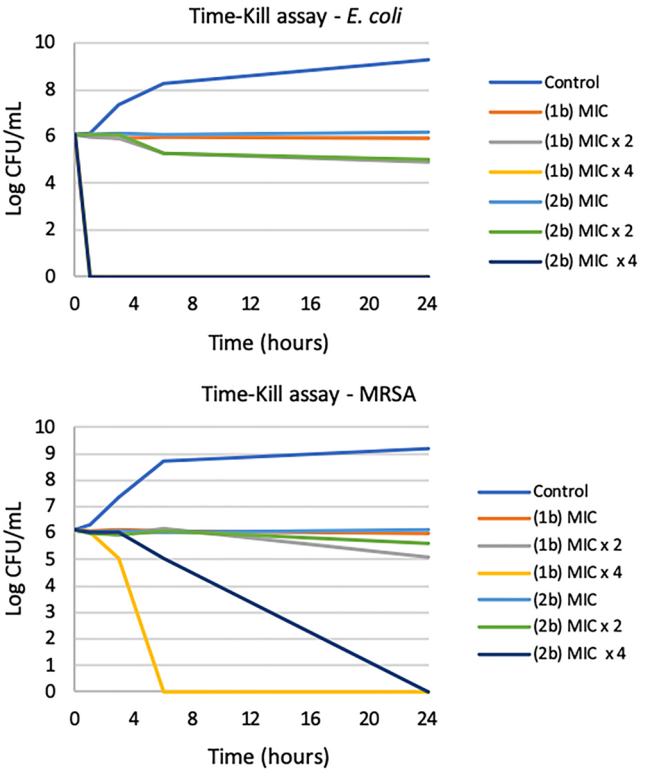


**Figure 5.** Time-kill assays of complexes **1b** and **2b** (at various concentrations) against *E. coli* (top) and MRSA (bottom).

**Bacterial Membrane Integrity (Scanning Electron Microscopy, SEM).** On the basis of the results of the uptake and time-kill assays, we were encouraged to further probe the mechanism by which the bismuth thiolates were killing bacterial cells, using SEM imaging. Complex **1b** was used as a representative example, and SEM images were captured of MRSA cells exposed to this complex at a range of different concentrations (MIC × $^1/_2$, MIC, MIC × 2, and MIC × 4) for 20 h. Untreated MRSA cells, used as a no additive control, remained morphologically intact, retaining their typical grape-like structures with smooth surfaces and no visible cell damage (Figure 6a). In contrast, cells exposed to complex **1b** (at all concentrations), looked visually unhealthy with distorted cell membranes (Figure 6b−e). As expected, at MIC × 4 concentrations, there was a significant decrease in the number of bacterial cells (viable and lysed) present on the surface, while the limited cells that did remain displayed a high degree of distortion in their cell shape. Surprisingly, and in contrast to time-kill assays, at MIC × 2, there was a significant reduction in the number of cells that remained after overnight exposure, and those that did remain visually looked impaired. Even at lower concentrations (sub-MIC and MIC), cells appeared morphologically unhealthy with bleb-like structures.[36] The increased abundance of extracellular debris, present on the surface of films exposed to **1b**, further suggests cell membrane destruction, and hence these SEM images are the first definitive evidence that bismuth(III) thiolate complexes interfere with bacterial membrane integrity.

Typically, highly lipophilic cell membrane targeting compounds act in a nonspecific detergent-like manner, which often excludes them for use as potential novel antibiotics.[37] Consequently, we wanted to address these potential selectivity concerns and assess the effect of bismuth thiolate complexes on the viability of mammalian cells.

**Mammalian Cell Cytotoxicity.** In attempting to develop novel antibacterial compounds, it is crucial that the inhibition of bacterial growth occurs at low compound concentrations, with high degrees of *selectivity* for prokaryotic cells over eukaryotic (mammalian) cells. All bismuth complexes were assessed against cos-7 cells using the CellTiter-Blue viability assay. The homoleptic bismuth(III) complexes, **3a−3l** ($BiL_3$), did not affect the cell viability up to concentrations of 50 $\mu$M. However, when cos-7 cells were exposed to the heteroleptic bismuth(III) thiolate complexes for 24 h (**1a−1l** and **2a−2g**), a significant reduction in the cellular viability was observed, with the half-maximal inhibition concentrations ($IC_{50}$) in the low micromolar range (Figure 7). Similar to the trends observed in the antibacterial assays, the monothiolate complexes **1a−1l** ($BiPh_2L$) showed generally lower $IC_{50}$ values (i.e., more significant reduction in the cellular viability) compared to the bisthiolate complexes (Figures 7 and 8). It is clear that the degree of thiolate substitution on the bismuth metal center has a marked influence on not only the antibacterial activity but also the mammalian cell toxicity.


https://dx.doi.org/10.1021/acs.inorgchem.9b03550
Inorg. Chem. XXXX, XXX, XXX−XXX

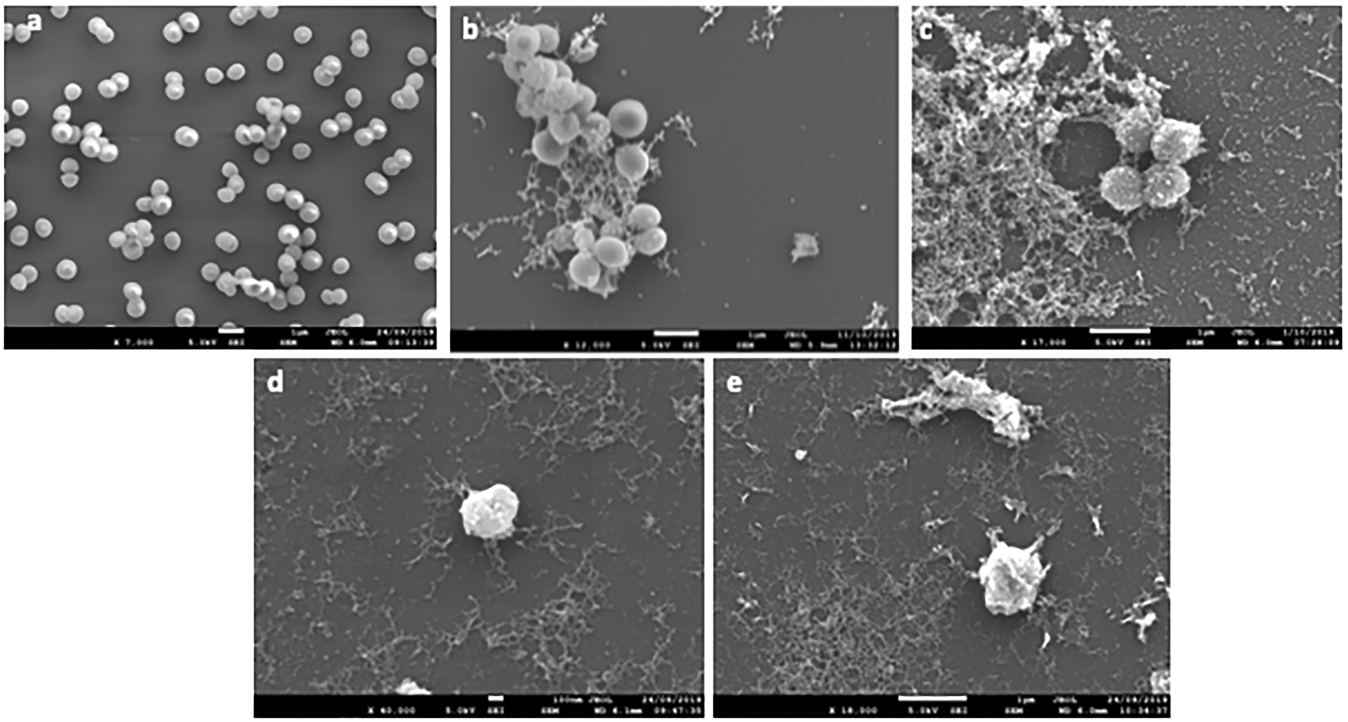


**Figure 6.** SEM images of (a) untreated MRSA cells and MRSA cells exposed to complex **1b** at (b) MIC × $^{1}/_{2}$, (c) MIC, (d) MIC × 2, and (e) MIC × 4. Scale bars: 1 $\mu$M (a–c and e) and 100 nm (d).

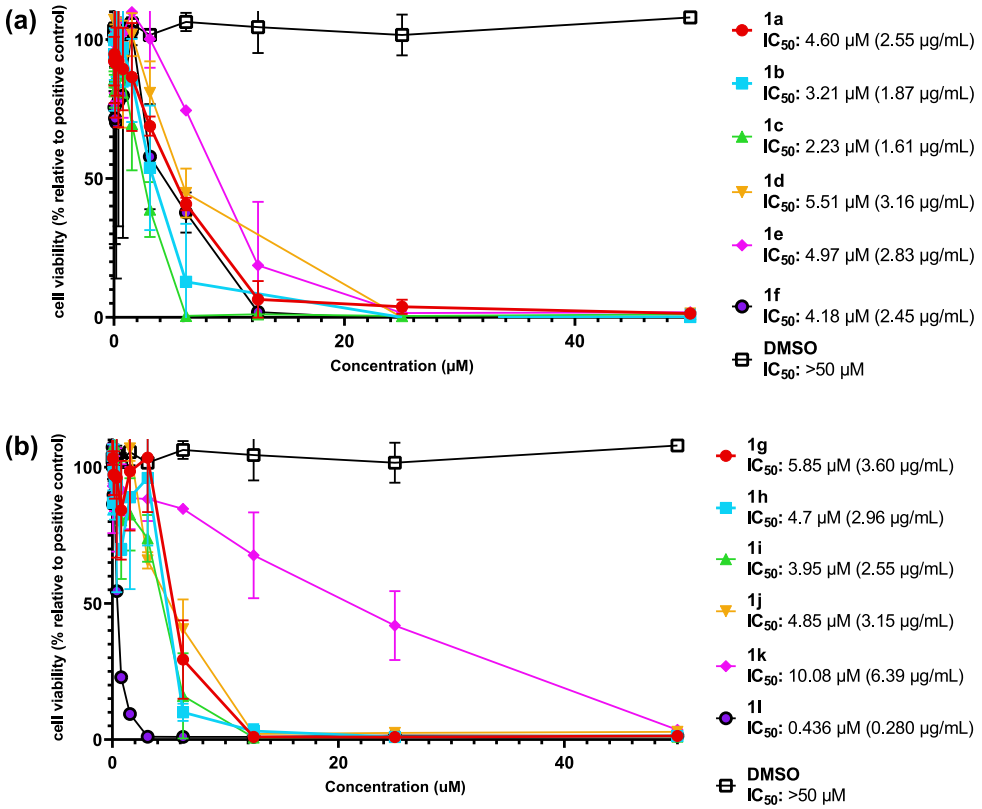


**Figure 7.** Comparison of percent cell viabilities of both tetrazole- and triazolethiolate complexes **1a–1l** ($BiPh_2L$) against cos-7 cells. Dose response curves were generated over a range of concentrations (24 nM to 50 $\mu$M) in the appropriate culture media from 10 mM DMSO stock solutions. All readings were compared spectroscopically to that of a nontreated control, and the percentage growth inhibition was calculated. A DMSO control was also included at the same range of concentrations.

On the basis of the cell viability studies, the trends show that there is little variation between the bismuth(III) triazole- and tetrazolethiolates. Small chemical changes in the thiolates show some structure–activity relationships. Interestingly, complex **1l**


https://dx.doi.org/10.1021/acs.inorgchem.9b03550
Inorg. Chem. XXXX, XXX, XXX–XXX

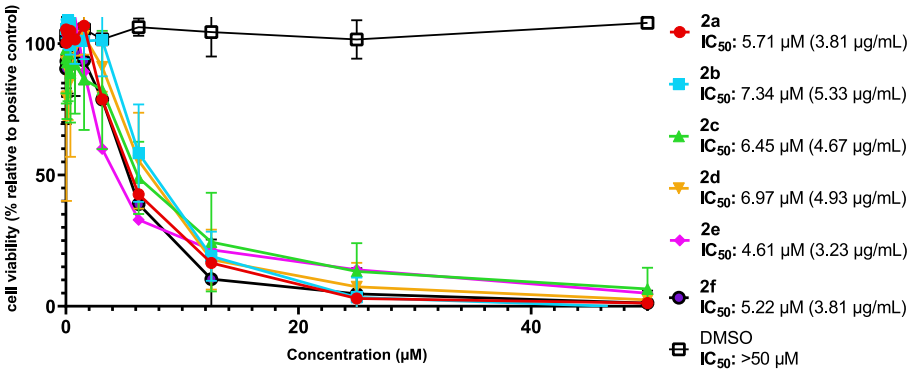


**Figure 8.** Comparison of percent cell viability of the tetrazolethiolate complexes **2a**–**2f** ($BiPhL_2$) against cos-7 cells. Dose response curves were generated over a range of concentrations (24 nM to 50 $\mu$M) in the appropriate culture media from 10 mM DMSO stock solutions. All readings were compared spectroscopically to that of a nontreated control, and the percentage growth inhibition was calculated. A DMSO control was also included at the same range of concentrations.

($IC_{50}$ = 0.44 $\mu$M), which contains two methyl groups, has an $IC_{50}$ value that is an order of magnitude more potent than any other complex reported. This could be a consequence of its apparent increase in lipophilicity (Table S2).

After assessment of both the antimicrobial activity and effect on the cell viability against cos-7 cells, it is vital to evaluate the ability of the complexes to selectivity inhibit pathogenic bacteria in the presence of mammalian cells. Consequently, the selectivity index (SI) values of all biologically active complexes have been calculated. SI is defined as the ratio between the antibacterial activity (MIC) and $IC_{50}$ against cos-7 cells, i.e., SI = $IC_{50}$/MIC. High SIs are favorable because they show a drug's potential to have a safe in vitro profile.[38] The SI values of complexes **1a**–**1l** and **2a**–**2f** using MRSA as the reference bacterial strain are shown in Table 2. The calculated SIs

**Table 2. SI Values of Complexes 1a–1l and 2a–2f**[a]

| complex | SI | complex | SI |
|---|---|---|---|
| **1a** | 1.63 | **1g** | 0.46 |
| **1b** | 1.19 | **1h** | 0.37 |
| **1c** | 0.83 | **1i** | 0.31 |
| **1d** | 2.03 | **1j** | 0.39 |
| **1e** | 1.81 | **1k** | 0.81 |
| **1f** | 0.78 | **1l** | 0.03 |
| **2a** | 1.22 | **2d** | 1.58 |
| **2b** | 1.71 | **2e** | 1.03 |
| **2c** | 1.50 | **2f** | 1.22 |

[a]The SI is calculated using the MICs against MRSA and the $IC_{50}$ values against cos-7 cells.

highlight the poor selectivity for bacterial cells that the bismuth(III) thiolate complexes (**1a**–**1l** and **2a**–**2f**) possess. In general, the SIs of bismuth tetrazole complexes **1a**–**1f** and **2a**–**2f** are just over 1, showing a small and nonsignificant affinity for bacterial cells over mammalian cells. Conversely, the bismuth triazole complexes **1g**–**1l** seem to display a greater affinity toward mammalian cos-7 cells, with complex **1l** being the most selectively cytotoxic. The aforementioned complex (**1l**) has an $IC_{50}$ value over 10 times lower than its respective MIC against MRSA. Accordingly, it can be concluded that the these bismuth(III) thiolate complexes possess such poor SIs that to consider them as novel antimicrobials without extensive structural modifications is highly implausible. The previously obtained SEM images, which point toward the cell membrane destruction of MRSA cells by bismuth(III) thiolates, could explain this poor selectivity. This is due to similarities in the membrane of bacteria and mammalian cells, which share many common structural and biochemical features.

**Determination of the Hemolytic Activity.** Due in large part to the rapid bactericidal activity displayed by the complexes in time-kill assays as well as the apparent cytotoxicity effects against cos-7 cells, complexes **1b**, **2b**, and **3b** as well as $BiPh_3$ were evaluated for their hemolytic activity against red blood cells at concentrations exceeding MIC × 4 for **1b** and **2b** (25 $\mu$g/mL). Trixton X-100 at 2% served as a positive control, while DMSO at 2% served as a negative control. The release of hemoglobin, measured at 540 nm, was used to quantify the membrane-damaging properties of the bismuth tetrazolethiolates. At this particular concentration (25 $\mu$g/mL), all three of the bismuth tetrazolethiolates (**1b**, **2b**, and **3b**) as well as $BiPh_3$ displayed no significant hemolytic activity[39] relative to the positive control (Figure 9).

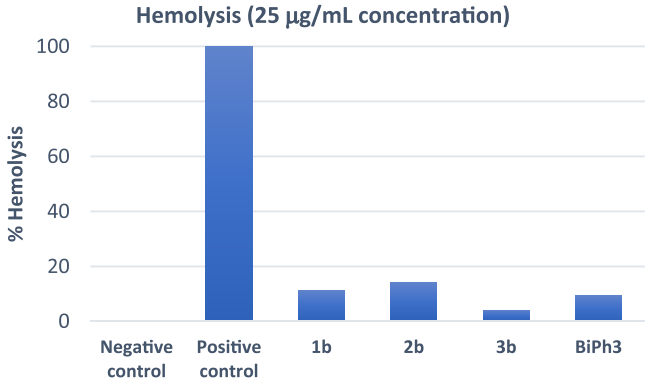


**Figure 9.** Percentage of hemolysis induced by complexes **1b**, **2b**, and **3b** and $BiPh_3$.

Interestingly, despite showing considerable cytotoxicity against cos-7 cells, the hemolytic activity of **1b** and **2b** suggests a much greater selectivity toward bacterial cells over mammalian cells. In comparison to the positive control (100% hemolysis), at 25 $\mu$g/mL complexes **1b** and **2b** caused only 11 and 14% hemolysis, respectively. The stark difference between the membrane-destructive effects of compounds against cos-7 cells and red blood cells is not uncommonly observed in the literature and has been attributed to the differences in the


https://dx.doi.org/10.1021/acs.inorgchem.9b03550
Inorg. Chem. XXXX, XXX, XXX−XXX

composition of the aforementioned membranes and their respective glycocalyx.[40] It can therefore be hypothesized that the biologically active bismuth(III) thiolates may have a higher affinity for bacterial and fibroblast-like cell membranes relative to the membrane of red blood cells. Conversely, the reduced time frame at which the red blood cells are exposed to the complexes (2 h) is much shorter than that in cytotoxicity (24 h) and bacterial (20 h) studies, and it may also be apparent that this has a significant effect on the reduced toxicity toward erythrocytes.

## CONCLUSION

Despite bismuth generally being considered to be nontoxic, we have demonstrated that its complexes should not be regarded as inherently safe just because of their metal center. The bismuth(III) thiolates detailed in this study demonstrate that the particular ligand class and number surrounding the metal center play significant roles in the cytotoxicity of these bismuth complexes. A total of 30 new bismuth(III) thiolates were synthesized from the reaction of tetrazole- and triazolethiols (thiones) with either $BiPh_3$, $BiPh_2Cl$, or $Bi(O^tBu)$. Preliminary antibacterial assays conducted on these compounds revealed that the degree of substitution around the bismuth metal center is key, with potent activity only seen for heteroleptic complexes ($BiPh_2L$ or $BiPhL_2$) containing either one or two azole ligands. Homoleptic complexes ($BiL_3$) with three tetrazole or triazole ligands coordinated to the metal center were shown to be completely inactive, and the results obtained from ICP-MS analysis suggest that this is a direct result of a decrease in their cellular uptake relative to their heteroleptic counterparts. Further mode of action studies conducted on a number of complexes point toward the cell membrane being the target site of action for bismuth(III) thiolates. The cell membranes of bacterial and mammalian cells share many common structural and biochemical characteristics. Hence, at this point in the drug discovery program, we became concerned that the bismuth(III) thiolates could have a nonspecific mode of action, resulting in cytotoxic effects and poor SIs. There are a plethora of compounds, both naturally derived and chemically synthesized, that can kill pathogenic bacteria, but many of these candidates often also perturb the membrane of mammalian cells. Subsequently, in vitro cell viability assays were conducted on bismuth(III) thiolates using cos-7 cells, which revealed their potent cytotoxic nature. The heteroleptic complexes that were shown to be active against bacteria were also shown to be cytotoxic, with no significant degree of selectivity for bacterial cells. However, in contrast, hemolytic assays were performed on a number of these complexes, and no significant hemolysis was observed. Consequently, this study has highlighted the importance of using a number of different in vitro cytotoxicity assays in the development of potentially novel pharmaceuticals. As was the case with bismuth(III) thiolates, new complexes can appear to be nontoxic (hemolysis assay) in some circumstances and considerably cytotoxic in others (CellTiter-Blue, cos-7). These findings highlight the complexities involved in determining the metal toxicity and raises the question of whether bismuth really is the green metal.

## EXPERIMENTAL SECTION

**Microbiology.** *Bacterial Growth.* MRSA (M118797, methicillin-resistant *S. aureus*), VRE (M846910, vancomycin-resistant *E. faecalis*), *P. aeruginosa* (ATCC27853), and *E. coli* (G102) were recovered from frozen (−80 °C) glycerol stocks (15% v/v) on either freshly prepared nutrient agar (Gram-positive) or LB agar (Gram-negative) at 37 °C for 24 h. Single colonies were then placed in either 3 mL of BHI media or LB media and incubated at 37 °C and 180 rpm for 18 h.

*Disk Diffusion.* The antibiotic activity of the synthesized complexes was determined using a Kirby−Bauer disk diffusion method. Briefly, 200 μL of a 1:100 dilution of overnight-cultured bacteria was applied to either nutrient agar or LB agar plates in order to form the confluent bacterial lawn. Sterile disks, inoculated with 60 μL of synthesized complexes, were then placed on the streaked agar plates before being incubated for 24 h at 37 °C. After incubation, the zone of inhibition (if it existed) was recorded and measured in millimeters.

*MIC.* The MIC of the synthesized complexes was determined using a broth microdilution method according to Clinical Standard Laboratory Institute (CSLI) guidelines. Briefly, 25 μL of a 1:100 dilution of an overnight culture of bacteria (to give approximately $5 \times 10^5$ CFU/mL) was added to falcon tubes containing 1 mL of serially diluted complexes in either BHI (Gram-positive) or LB (Gram-negative) media. The MIC was determined as the lowest concentration of complex where visible growth of the bacteria was inhibited following overnight incubation (37 °C, 180 rpm) for 20 h.

*Time-Kill Assay.* The mode of inhibitory activity of the synthesized complexes was determined by measuring the decrease in the CFU with time. First, an overnight culture of bacteria was centrifuged for 15 min at 4000 rpm and washed three times with 1 mL of PBS. The bacterial pellets were resuspended in either BHI or LB and diluted to approximately $5 \times 10^5$ CFU/mL before varying concentrations of complexes were added and incubated at 37 °C and 180 rpm. Bacterial survivors were determined by plating serial dilutions onto agar plates at 0, 1, 3, 6, and 24 h after incubation.

*SEM.* The cell morphology of MRSA cells exposed to bismuth complexes was analyzed by SEM. A single colony of MRSA was added to a falcon tube containing 3 mL of BHI broth and incubated overnight at 37 °C and 180 rpm. The overnight-cultured bacteria was then diluted to approximately $5 \times 10^5$ CFU/mL before complexes were added and incubated overnight at 37 °C and 180 rpm for a further 20 h. Following overnight incubation, the bacterial solutions were centrifuged at 4000 rpm for 15 min, with the supernatant discarded for use. Pelleted cells were first washed three times with 1 mL of PBS before being fixed in 2.5% glutaraldehyde and 2% paraformaldehyde (in 0.1 M sodium cacodylate buffer) for 1 h at room temperature. The fixed cells were then washed three times in a fresh sodium cacodylate buffer before being post-fixed in 1% osmium tetroxide in a cacodylate buffer at room temperature. Post-fixed cells were washed three times with Milli-Q water, and 100 μL aliquots were incubated on round coverslips coated with 0.1% polyethylenimine for 45 min. Following incubation, excess cells were washed off by immersing the coverslips in water, and the coverslips with adhered cells were then dehydrated in increasing concentrations of ethanol, consisting of 30, 50, 70, 90, and 2 × 100% ethanol for 10 min each. Dehydrated cells on the coverslips were dried with a Bal-Tec CPD 030 critical point drier. The coverslips were then mounted, using carbon adhesive tape, onto SEM specimen stubs before being coated with iridium. Analyses were carried out on a JEOL JSM-7001F field-emission-gun scanning electron microscope.

*Cell Uptake Assay.* Overnight cultures of MRSA and *E. coli* were first diluted to approximately $1 \times 10^6$ CFU/mL and added to falcon tubes containing the complexes diluted in BHI so that the overall concentration of the active components was 5.3 μM (for complexes **1f**, **2f**, and **3f**) and 12.5 μM (for complexes **1i** and **3i**) in solution. After incubation for 20 h (37 °C, 180 rpm), the falcon tubes were centrifuged for 15 min at 4000 rpm, with the resulting supernatant discarded. The leftover pelleted cells were then washed six times with 1 mL of PBS before being resuspended in 3 mL of BHI in order to determine the CFU/mL of bacteria present (serial dilution and overnight incubation of nutrient agar plates). The falcon tubes were then recentrifuged (15 min, 4000 rpm) and the pelleted bacteria washed a further six times with 1 mL of PBS before 200 μL of concentrated $HNO_3$ was added and left to sit at 60 °C overnight. The


https://dx.doi.org/10.1021/acs.inorgchem.9b03550
Inorg. Chem. XXXX, XXX, XXX−XXX

solutions were then diluted with 4.8 mL of 2% $HNO_3$ before the $Bi^{209}$ composition was measured by ICP-MS.

*ICP-MS.* Determination of the bismuth content following uptake experiments was conducted using a PerkinElmer NexION 350 inductively coupled plasma mass spectrometer, measuring bismuth at 208.98 amu. Raw count rates from the analyses were externally standardized by means of a calibration curve constructed using a commercially available bismuth stock solution. An internal standard of 80 ppb lead was used for bismuth analysis. The precision is on the order of <5% relative standard deviation from the single analyses. The final bismuth content was averaged from three independent bacterial experiments.

*Cell Viability Assay (Cytotoxicity).* All media and supplements were purchased from Gibco and maintained as directed. Cos-7 cells were cultured in Dulbecco's modified Eagle's medium previously supplemented with 1% penicillin/streptomycin, 1% glutamax, and 10% fetal bovine serum. The cells were maintained at 37 °C in a 5% $CO_2$ incubator. A CellTiter-Blue Cell Viability Assay kit was purchased from Promega Corp. and used to determine the effect that bismuth complexes had on the viability of cos-7 cells.

Falcon 96-well flat-bottom plates were initially seeded at $10^5$ cells/mL with adherent cos-7 cells for 24 h. Compounds **1a−1l**, **2a−2h**, and **3a−3l** were then dissolved in DMSO to make up a 10 mM working stock and sequentially diluted out in the appropriate culture media (50 $\mu$M to 24 nM). Following the addition of compounds to the adherent cells, plates were incubated for an additional 24 h. CellTiter-Blue was added to the plates at 15% total well volume according to the manufacturer's protocol. Assays were then measured spectroscopically using fluorescence excitation at 544 nm and emission at 590 nm to determine the cell viability. The compounds were compared to a no-drug negative control as well as a positive control of untreated cells to determine the percent inhibition and percent viability calculated. Fluorescence measurements were conducted on a BMG-Labtech ClarioStar microplate reader. Three independent assays were conducted for each compound. Standard deviations and $IC_{50}$ values were modeled through a nonlinear regression (curve fit) on the GraphPad *Prism 8* program.

*Hemolysis Assay.* Hemolysis assays were performed as detailed by Ciornei et al.[40] Blood was first centrifuged at 800*g* for 10 min before the supernatant and buffy coat layer were discarded before for use. This step was repeated a further two times before the resulting erythrocytes were resuspended in PBS (5% v/v). Next, complexes (overall concentration = 25 $\mu$g/mL) were added to individual PCR tubes containing 1.5 mL of the erythrocytes and incubated for 2 h at 37 °C with gentle end-overend rotation. 2% Trixton X-100 served as a positive control, while 2% DMSO served as a negative control. After incubation, the samples were centrifuged at 800*g* for 10 min. The percent hemolysis was determined by measuring the absorbance of the supernatant (release of hemoglobin) at 540 nm and expressed as a percentage of the positive control's induced hemolysis.

**Chemistry.** $BiPh_3$[13] and $Bi(O^tBu)_3$[41] were synthesized following literature procedures. Starting materials for the synthesis of thiols were purchased from the commercial supplies Sigma-Aldrich and Oakwood Chemicals. BHI broth was obtained from Oxoid Australia Pty. $^1H$ and $^{13}C$ NMR spectra were recorded on a Bruker AV600 or Bruker AV400 spectrometer at 600 and 125 MHz or 400 and 100 MHz, respectively. Chemical shifts are quoted in parts per million (ppm) and are referenced to the residual solvent peak (DMSO). IR spectroscopy measurements were carried out with a Cary 630 Fourier transform infrared spectrometer in the range of 4000−500 $cm^{-1}$. Mass spectrometry was performed on a Micromass Platform QMS spectrometer with an electrospray source and a cone voltage of 35 eV. Melting points were obtained using a Stuart Scientific SMP 3 melting point machine. Elemental analysis was carried out by Dr. Biplop Saha at Monash University.

**General Procedures (GP).** *GP1: Heteroleptic Monotetrazolebisphenylbismuth(III) Complex Synthesis.* All of the following manipulations were carried out using a CEM discover LabMate microwave as follows: $BiPh_3$ (1.2 equiv) was first dissolved in 5 mL of methanol before the previously synthesized tetrazolethiolate ligand (1 equiv) was added. The resulting solution was reacted at 70 °C for 20 min before being left to cool to room temperature. Upon cooling, the desired compound crashed out of the solution as pure crystalline solids, which were filtered and collected without the need for further purification.

*GP2: Heteroleptic Monotriazolebisphenylbismuth(III) Complex Synthesis.* All of the following manipulations were carried out under a nitrogen atmosphere using Schlenk techniques. $BiPh_2Cl$ (1 equiv) was added to a solution of the previously synthesized triazole (1 equiv) with NaOH (1 equiv) in dry methanol. The resulting solution was stirred at room temperature for 4 h. After the elapsed time, the precipitate that formed was filtered and washed with cold water and acetone to yield the desired complex.

*GP3: Heteroleptic Bistetrazolemonophenylbismuth(III) Complex Synthesis.* All of the following manipulations were carried out using a CEM discover LabMate microwave as follows: $BiPh_3$ (1 equiv) was first dissolved in 5 mL of methanol before the previously synthesized tetrazolethiolate ligand (2.2 equiv) was added. The resulting solution was reacted at 50 °C for 40 min before being left to cool to room temperature. After subsequent cooling for 2 h, impurities that crashed out of the solution were removed by filtration, with the resulting filtrate concentrated in vacuo. The remaining crude mixture was then washed with cold diethyl ether to remove any unreacted $BiPh_3$, with the leftover solid being the desired complex.

*GP4: Homoleptic Tetrazole/triazolebismuth(III) Complex Synthesis.* All of the following manipulations were carried out under a nitrogen atmosphere using Schlenk techniques. $Bi(O^tBu)_3$ (1 equiv) was added to a solution of the tetrazole/triazolethiolate (3 equiv) in dry THF at room temperature. The resulting solution was allowed to stir overnight before being concentrated in vacuo. The crude solid obtained was washed with cold diethyl ether and filtered to yield the desired compound.

*$[Bi(Ph)_2(C_8H_7N_4S)]$ (**1a**).* Following GP1, 1-(*p*-tolyl)-1*H*-tetrazole-5-thiol (90 mg, 0.47 mmol) and $BiPh_3$ (247 mg, 0.56 mmol) were stirred in 7 mL of methanol. The title compound was isolated as light-orange crystals (190 mg, 73%). $^1H$ NMR (400 MHz, DMSO-$d_6$): $\delta$ 8.30−8.23 (m, 4H), 7.59 (t, $J$ = 7.4 Hz, 4H), 7.55−7.49 (m, 2H), 7.39−7.33 (m, 4H), 2.37 (s, 3H). $^{13}C$ NMR (101 MHz, DMSO-$d_6$): $\delta$ 157.6, 139.2, 137.8, 137.3, 132.0, 131.3, 130.3, 129.8, 127.7, 124.3, 20.7. IR (film, $cm^{-1}$): $\nu$ 3047 (C−H), 1370 (C−N), 821 (C−S). Mp: 184−186 °C. MS (ESI). Calcd for $C_{20}H_{17}BiN_4S$: $m/z$ 555.1059 [$(M + H)^+$]. Elem anal. Calcd C, 43.31; H, 3.09; N, 10.11. Found: C, 43.58; H, 2.96; N, 10.00. CCDC 1968625.

*$[Bi(Ph)_2(C_9H_{10}N_5S)]$ (**1b**).* Following GP1, 1-(4-dimethylamino)-phenyl)-1*H*-tetrazole-5-thiol (100 mg, 0.45 mmol) and $BiPh_3$ (237 mg, 0.54 mmol) were stirred in 7 mL of methanol. The title compound was isolated as light-orange crystals (150 mg, 57%). $^1H$ NMR (400 MHz, DMSO-$d_6$): $\delta$ 8.28−8.23 (m, 4H), 7.58 (dd, $J$ = 8.2 and 7.0 Hz, 4H), 7.40−7.31 (m, 4H), 6.82−6.76 (m, 2H), 2.95 (s, 6H). $^{13}C$ NMR (101 MHz, DMSO-$d_6$): $\delta$ 157.3, 150.6, 137.8, 137.3, 131.3, 130.3, 127.7, 125.4, 122.8, 111.8. IR (film, $cm^{-1}$): $\nu$ 3048 (C−H), 1371 (C−N), 822 (C−S). Mp: 159 °C. MS (ESI). Calcd for $C_{21}H_{20}BiN_5S$: $m/z$ 584.1423 [$(M + H)^+$]. Elem anal. Calcd: C, 43.23; H, 3.40; N, 12.00. Found: C, 42.9; H, 3.13; N, 11.95. CCDC 1968624.

*$[Bi(Ph)_2(C_{10}H_{11}N_4S)]$ (**1c**).* Following GP1, 1-mesityl-1*H*-tetrazole-5-thiol (100 mg, 0.45 mmol) and $BiPh_3$ (237 mg, 0.54 mmol) were stirred in 7 mL of methanol. The title compound was isolated as pale-yellow crystals (163 mg, 63%). $^1H$ NMR (400 MHz, DMSO-$d_6$): $\delta$ 8.27−8.20 (m, 4H), 7.57 (dd, $J$ = 8.3 and 6.9 Hz, 4H), 7.38−7.31 (m, 2H), 7.08−7.03 (m, 2H), 2.31 (s, 3H), 1.79 (s, 6H). $^{13}C$ NMR (101 MHz, DMSO-$d_6$): $\delta$ 140.0, 137.6, 137.3, 135.1, 131.2, 130.3, 130.1, 129.0, 127.7, 20.6, 16.9. IR (film, $cm^{-1}$): $\nu$ 3062 (C−H), 1368 (C−N), 856 (C−S). Mp: 173 °C. MS (ESI). Calcd for $C_{22}H_{21}BiN_4S$: $m/z$ 505.0855 $(PhBiL)^+$. Elem anal. Calcd C, 45.37; H, 3.63; N, 9.62. Found: C, 45.39; H, 3.45; N, 9.63.

*$[Bi(Ph)_2(C_7H_4ClN_4S)]$ (**1d**).* Following GP1, 1-(4-chlorophenyl)-1*H*-tetrazole-5-thiol (50 mg, 0.23 mmol) and $BiPh_3$ (125 mg, 0.28 mmol) were stirred in 5 mL of methanol. The title compound was isolated as light-orange crystals (100 mg, 79%). $^1H$ NMR (400 MHz, DMSO-


https://dx.doi.org/10.1021/acs.inorgchem.9b03550
Inorg. Chem. XXXX, XXX, XXX−XXX

$d_6$): δ 8.31−8.24 (m, 4H), 7.75−7.70 (m, 2H), 7.66−7.56 (m, 6H), 7.36 (td, $J$ = 7.4 and 1.4 Hz, 2H). $^{13}$C NMR (151 MHz, DMSO-$d_6$): δ 158.0, 137.8, 133.9, 133.3, 131.4, 130.3 129.5, 127.8, 126.1. IR (film, cm$^{-1}$): ν 3047 (C−H), 1368 (C−N), 833 (C−S). Mp: 171−173 °C. MS (ESI). Calcd for $C_{19}H_{14}BiClN_4S$: $m/z$ 597.0326 [(M + Na)$^+$]. Elem anal. Calcd: C, 39.70; H, 2.45; N, 9.75. Found: C, 39.41; H, 2.49; N, 9.75. CCDC 1968616.

*[Bi(Ph)$_2$(C$_8$H$_7$ON$_4$S)] (**1e**).* Following GP1, 1-(4-methoxyphenyl)-1*H*-tetrazole-5-thiol (50 mg, 0.22 mmol) and $BiPh_3$ (115 mg, 0.26 mmol) were stirred in 5 mL of methanol. The crude solid present after the reaction was filtered and then washed with cold diethyl ether to yield the desired compound as a pale-yellow solid (100 mg, 80%). $^1$H NMR (400 MHz, DMSO-$d_6$): δ 8.30−8.24 (m, 4H), 7.62−7.52 (m, 6H), 7.35 (ddt, $J$ = 8.8, 7.3, and 1.4 Hz, 2H), 7.12−7.07 (m, 2H), 3.82 (s, 3H). $^{13}$C NMR (101 MHz, DMSO-$d_6$): δ 159.7, 137.8, 131.3, 127.7, 127.2, 126.1, 114.5, 55.6. IR (film, cm$^{-1}$): ν 3008 (C−H), 1367 (C−N), 833 (C−S). Mp: 151 °C. MS (ESI). Calcd for $C_{20}H_{17}BiN_4OS$: $m/z$ 593.0826 [(M + Na)$^+$]. Elem anal. Calcd: C, 42.11; H, 3.00; N, 9.82. Found: C, 41.83; H, 2.97; N, 10.04.

*[Bi(Ph)$_2$(C$_7$H$_4$O$_2$N$_5$S)] (**1f**).* Following GP1, 1-(4-nitrophenyl)-1*H*-tetrazole-5-thiol (60 mg, 0.27 mmol) and $BiPh_3$ (142 mg, 0.32 mmol) were stirred in 5 mL of methanol. The crude solid present after the reaction was filtered and then washed with cold diethyl ether to yield the desired compound as a pale-yellow solid (78 mg, 49%). $^1$H NMR (400 MHz, DMSO-$d_6$): δ 8.42−8.38 (m, 2H), 8.29 (dt, $J$ = 7.7 and 1.3 Hz, 4H), 8.14 (d, $J$ = 8.7 Hz, 2H), 7.62 (t, $J$ = 7.5 Hz, 4H), 7.37 (tt, $J$ = 7.3 and 1.3 Hz, 2H). $^{13}$C NMR (151 MHz, DMSO-$d_6$): δ 158.7, 147.0, 139.4, 137.8, 137.3, 131.4, 130.3, 127.8, 124.9, 124.8. IR (film, cm$^{-1}$): ν 3046 (C−H), 1346 (C−N), 852 (C−S). Mp: 175 °C (dec). MS (ESI). Calcd for $C_{19}H_{14}BiN_5O_2S$: $m/z$ 586.0750 [(M + H)$^+$]. Elem anal. Calcd C, 38.98; H, 2.41; N, 11.96. Found: C, 38.75; H, 2.05; N, 12.04. CCDC 1968617.

*[Bi(Ph)$_2$(C$_{13}$H$_9$N$_4$S)] (**1g**).* Following GP2, $BiPh_2Cl$ (200 mg, 0.5 mmol) was reacted with triazolethiol **g** (138 mg, 0.5 mmol) in methanol. The title complex was isolated as an off-white solid (302 mg, 98%). $^1$H NMR (400 MHz, DMSO-$d_6$): δ 8.52 (d, $J$ = 6.2 Hz, 2H), 8.24 (d, $J$ = 7.3 Hz, 4H), 7.54 (t, $J$ = 7.6 Hz, 4H), 7.35−7.28 (m, 1H), 7.28−7.18 (m, 2H), 7.03 (d, $J$ = 8.9 Hz, 1H). $^{13}$C NMR (151 MHz, DMSO-$d_6$): δ 149.9, 137.9, 135.2, 134.7, 131.1, 129.7, 129.5, 127.9, 127.5, 121.0. IR (film, cm$^{-1}$): ν 1599 (C═C), 1428 (C−N), 1342 (C−N), 832 (C−S), 722 (C−C). Mp: 214−219 °C. MS (ESI). Calcd for $C_{25}H_{19}BiN_4S$: $m/z$ 645.1505 [(M + H)$^+$]. CCDC 1968621.

*[Bi(Ph)$_2$(C$_{14}$H$_{11}$N$_4$S)] (**1h**).* Following GP2, $BiPh_2Cl$ (200 mg, 0.5 mmol) was reacted with triazolethiol **h** (145 mg, 0.5 mmol) in methanol. The title complex was isolated as an off-white solid (274 mg, 87%). $^1$H NMR (400 MHz, DMSO-$d_6$): δ 8.52 (d, $J$ = 6.2 Hz, 2H), 8.24 (d, $J$ = 7.3 Hz, 4H), 7.54 (t, $J$ = 7.6 Hz, 4H), 7.35−7.28 (m, 1H), 7.28−7.18 (m, 2H), 7.03 (d, $J$ = 8.9 Hz, 1H). $^{13}$C NMR (151 MHz, DMSO-$d_6$): δ 150.0, 137.8, 137.3, 131.1, 130.3, 130.2, 127.6, 127.6, 121.0. IR (film, cm$^{-1}$): ν 1575 (C═C), 1460 (C−N), 1390 (C−N), 824 (C−S), 735 (C−H). Mp: 161−162 °C. MS (ESI). Calcd for $C_{25}H_{19}BiN_4S$: $m/z$ 645.1507 [(M + H)$^+$]. CCDC 1968619.

*[Bi(Ph)$_2$(C$_{14}$H$_{11}$N$_4$OS)] (**1i**).* Following GP2, $BiPh_2Cl$ (200 mg, 0.5 mmol) was reacted with triazolethiol **i** (153 mg, 0.5 mmol) in methanol. The title complex was isolated as an off-white solid (273 mg, 85%). $^1$H NMR (400 MHz, DMSO-$d_6$): δ 8.59−8.45 (m, 2H), 8.24 (d, $J$ = 7.3 Hz, 4H), 7.54 (t, $J$ = 7.6 Hz, 4H), 7.41−7.28 (m, 2H), 7.29−7.17 (m, 4H), 7.03 (d, $J$ = 8.9 Hz, 2H), 3.80 (s, 3H). $^{13}$C NMR (151 MHz, DMSO-$d_6$): δ 150.0, 137.8, 131.1, 128.3 (d, $J$ = 236.8 Hz), 121.0, 114.8, 55.5. IR (film, cm$^{-1}$): ν 1575 (C═C), 1460 (C−N), 1390 (C−N), 824 (C−S), 735 (C−H). Mp: 119−123 °C. Elem anal. Calcd C, 48.30; H, 3.27; N, 8.67. Found: C, 48.95; H, 3.33; N, 8.69. MS (ESI). Calcd for $C_{25}H_{19}BiN_4S$: $m/z$ 647.1302 [(M + H)$^+$].

*[Bi(Ph)$_2$(C$_{13}$H$_8$N$_4$ClS)] (**1j**).* Following GP2, $BiPh_2Cl$ (200 mg, 0.5 mmol) was reacted with triazolethiol **j** (155 mg, 0.5 mmol) in methanol. The title complex was isolated as an off-white solid (173 mg, 53%). $^1$H NMR (400 MHz, DMSO-$d_6$): δ 8.52 (d, $J$ = 6.2 Hz, 4H), 8.26 (d, $J$ = 7.3 Hz, 2H), 7.55 (dd, $J$ = 8.2 and 6.1 Hz, 5H), 7.33 (dd, $J$ = 8.1 and 6.0 Hz, 3H), 7.29−7.15 (m, 2H). $^{13}$C NMR (151 MHz, DMSO-$d_6$): δ 131.7, 130.3, 114.8. IR (film, cm$^{-1}$): ν 1575 (C═C), 824 (C−S), 735 (C−H). Mp: 119−123 °C (dec). MS (ESI). Calcd for $C_{25}H_{19}BiClN_4S$: $m/z$ 650.0735 [(M + Na)$^+$]. Elem anal. Calcd: C, 46.13; H, 2.79; N, 8.61. Found: C, 44.95; H, 2.64; N, 8.47.

*[Bi(Ph)$_2$(C$_{13}$H$_8$N$_4$FS)] (**1k**).* Following GP2, $BiPh_2Cl$ (200 mg, 0.5 mmol) was reacted with triazolethiol **k** (148 mg, 0.5 mmol) in methanol. The title complex was isolated as an off-white solid (121 mg, 38%). $^1$H NMR (600 MHz, DMSO-$d_6$): δ 8.56−8.46 (m, 1H), 8.25 (dd, $J$ = 7.8 and 1.4 Hz, 2H), 7.56 (t, $J$ = 7.6 Hz, 2H), 7.42−7.30 (m, 2H), 7.25−7.15 (m, 1H). $^{13}$C NMR (151 MHz, DMSO-$d_6$): δ 150.0, 137.8, 131.2, 127.6, 121.2, 116.7, 116.6. IR (film, cm$^{-1}$): ν 1575 (C═C), 1460 (C−N), 824 (C−S), 735 (C−H). Mp: 121 °C (dec). MS (ESI). Calcd for $C_{25}H_{19}BiFN_4S$: $m/z$ 635.10782 [(M + H)$^+$]. CCDC 1968620.

*[Bi(Ph)$_2$(C$_{15}$H$_{13}$N$_4$S)] (**1l**).* Following GP2, $BiPh_2Cl$ (200 mg, 0.5 mmol) was reacted with triazolethiol **l** (152 mg, 0.5 mmol) in methanol. The title complex was isolated as an off-white solid (242 g, 75%). $^1$H NMR (600 MHz, DMSO-$d_6$): δ 8.49 (d, $J$ = 6.2 Hz, 1H), 8.35−8.18 (m, 3H), 7.52 (t, $J$ = 7.5 Hz, 3H), 7.36−7.26 (m, 2H), 7.21 (dd, $J$ = 4.4 and 1.8 Hz, 2H), 7.19−7.13 (m, 1H), 7.10 (d, $J$ = 7.9 Hz, 1H), 2.34 (s, 2H), 1.83 (s, 2H). $^{13}$C NMR (151 MHz, DMSO-$d_6$): δ 150.1, 137.9, 134.8 (d, $J$ = 40.2 Hz), 131.9, 128.2 (d, $J$ = 38.6 Hz), 127.5, 120.0. IR (film, cm$^{-1}$): ν 1575 (C═C), 1460 (C−N), 824 (C−S), 735 (C−H). Mp: 161−162 °C. MS (ESI). Calcd for $C_{27}H_{23}BiN_4S$: $m/z$ 645.1507 [(M + H)$^+$]. CCDC 1968623.

*[Bi(Ph)(C$_8$H$_7$N$_4$S)$_2$] (**2a**).* Following GP3, 1-(*p*-tolyl)-1*H*-tetrazole-5-thiol (75 mg, 0.39 mmol) and $BiPh_3$ (68 mg, 0.16 mmol) were stirred in 4 mL of methanol. After the crashed-out solids were filtered off, the crude mixture was purified by HPLC and then concentrated in vacuo to yield the desired complex as a pale-yellow solid (35 mg, 33%). $^1$H NMR (600 MHz, DMSO-$d_6$): δ 8.90 (d, $J$ = 7.1 Hz, 2H), 7.85 (t, $J$ = 7.5 Hz, 2H), 7.58 (d, $J$ = 7.9 Hz, 4H), 7.43 (dd, $J$ = 8.0 and 6.6 Hz, 1H), 7.37 (d, $J$ = 8.1 Hz, 4H), 2.39 (s, 6H). $^{13}$C NMR (151 MHz, DMSO): δ 139.4, 139.1, 133.0, 132.0, 131.3, 129.7, 127.6, 124.3, 20.7. IR (film, cm$^{-1}$): ν 2922 (C−H), 1375 (C−N), 853 (C−S). Mp: 147−150 °C (dec). MS (ESI). Calcd for $C_{22}H_{19}BiN_8S_2$: $m/z$ 667.0849 [(M − H)$^-$].

*[Bi(Ph)(C$_9$H$_{10}$N$_5$S)$_2$] (**2b**).* Following GP3, 1-(4-dimethylamino)-phenyl)-1*H*-tetrazole-5-thiol (50 mg, 0.22 mmol) and $BiPh_3$ (45 mg, 0.10 mmol) were stirred in 4 mL of methanol. After the crashed-out solids were filtered off, the crude leftover mixture was triturated with methanol, with the remaining solids being the desired complex, isolated as a dark-yellow solid (29 mg, 40%). $^1$H NMR (400 MHz, DMSO-$d_6$): δ 8.91−8.84 (m, 2H), 7.83 (t, $J$ = 7.7 Hz, 2H), 7.42 (tt, $J$ = 7.4 and 1.3 Hz, 1H), 7.33−7.26 (m, 4H), 6.78−6.73 (m, 4H), 2.95 (s, 12H). $^{13}$C NMR (151 MHz, DMSO-$d_6$): δ 151.1, 139.8, 133.4, 128.1, 125.9, 123.1, 112.1. IR (film, cm$^{-1}$): ν 2890 (C−H), 1357 (C−N), 843 (C−S). Mp: 180−182 °C. MS (ESI). Calcd for $C_{24}H_{25}BiN_{10}S_2$: $m/z$ 761.1170 [(M + Cl)$^-$].

*[Bi(Ph)(C$_{10}$H$_{11}$N$_4$S)$_2$] (**2c**).* Following GP3, 1-mesityl-1*H*-tetrazole-5-thiol (100 mg, 0.45 mmol) and $BiPh_3$ (90 mg, 0.21 mmol) were stirred in 5 mL of methanol. After the crashed-out solids were filtered off, the crude mixture was purified by HPLC and then concentrated in vacuo to yield the desired complex as a yellow solid (52 mg, 34%). $^1$H NMR (600 MHz, DMSO-$d_6$): δ 8.84 (dd, $J$ = 7.8 and 1.5 Hz, 2H), 7.77 (t, $J$ = 7.7 Hz, 2H), 7.38 (ddd, $J$ = 8.9, 6.4, and 2.7 Hz, 1H), 7.05 (s, 4H), 2.30 (s, 6H), 1.77 (s, 12H). $^{13}$C NMR (101 MHz, DMSO-$d_6$): δ 140.5, 139.9, 135.5, 133.3, 130.6, 129.4, 128.0, 21.1, 17.4. IR (film, cm$^{-1}$): ν 2919 (C−H), 1374 (C−N), 851 (C−S). Mp: 134 °C. MS (ESI). Calcd for $C_{26}H_{27}BiN_8S_2$: $m/z$ 759.1292 [(M + Cl)$^-$]. Elem anal. Calcd: C, 43.09; H, 3.76; N, 15.46. Found: C, 42.93; H, 3.45; N, 15.72. CCDC 1968618.

*[Bi(Ph)(C$_7$H$_4$ClN$_4$S)$_2$] (**2d**).* Following GP3, 1-(4-chlorophenyl)-1*H*-tetrazole-5-thiol (80 mg, 0.36 mmol) and $BiPh_3$ (74 mg, 0.17 mmol) were stirred in 5 mL of methanol. After the crashed-out solids were filtered off, the crude leftover mixture was triturated with methanol, with the remaining solids being the desired complex, isolated as a yellow solid (42 mg, 35%). $^1$H NMR (600 MHz, DMSO-$d_6$): δ 8.92−8.89 (m, 2H), 7.86 (t, $J$ = 7.6 Hz, 2H), 7.70−7.66 (m, 4H), 7.62−7.59 (m, 4H), 7.44 (tt, $J$ = 7.3 and 1.3 Hz, 1H). $^{13}$C NMR (151 MHz,


https://dx.doi.org/10.1021/acs.inorgchem.9b03550
Inorg. Chem. XXXX, XXX, XXX−XXX

DMSO-$d_6$): δ 139.8, 134.2, 133.8, 133.6, 129.8, 128.8, 128.2, 126.4. IR (film, $cm^{-1}$): ν 3056 (C−H), 1371 (C−N), 836 (C−S). Mp: 174−176 °C. MS (ESI). Calcd for $C_{20}H_{13}BiCl_2N_8S_2$: *m/z* 742.9615 [(M + Cl)$^-$]. Elem anal. Calcd: C, 33.86; H, 1.85; N, 15.80. Found: C, 34.09; H, 1.67; N, 15.52. CCDC 1968622.

*[Bi(Ph)($C_8H_7ON_4S)_2$] **(2e)***. Following GP3, 1-(4-methoxyphenyl)-1*H*-tetrazole-5-thiol (80 mg, 0.34 mmol) and $BiPh_3$ (70 mg, 0.16 mmol) were stirred in 5 mL of methanol. After the crashed-out solids were filtered off, the crude mixture was purified by HPLC and then concentrated in vacuo to yield the desired complex as a yellow solid (47 mg, 42%). $^1$H NMR (400 MHz, DMSO-$d_6$): δ 8.89 (dd, *J* = 7.8 and 1.4 Hz, 2H), 7.84 (t, *J* = 7.6 Hz, 2H), 7.50−7.45 (m, 4H), 7.42 (tt, *J* = 7.4 and 1.3 Hz, 1H), 7.08−7.02 (m, 4H), 3.81 (s, 6H). IR (film, $cm^{-1}$): ν 2998 (C−H), 1368 (C−N), 848 (C−S). Mp: 170 °C (dec). MS (ESI). Calcd for $C_{22}H_{19}BiN_8O_2S_2$: *m/z* 737.0593 [(M + Cl)$^-$]. Elem anal. Calcd: C, 37.72; H, 2.73; N, 16.00. Found: C, 37.80; H, 2.69; N, 15.64.

*[Bi(Ph)($C_7H_4O_2N_5S)_2$] **(2f)***. Following GP3, 1-(4-nitrophenyl)-1*H*-tetrazole-5-thiol (95 mg, 0.42 mmol) and $BiPh_3$ (75 mg, 0.17 mmol) were stirred in 5 mL of methanol. After the crashed-out solids were filtered off, the crude leftover mixture was washed with cold diethyl ether, with the remaining solids being the desired complex, isolated as a yellow solid (72 mg, 36%). $^1$H NMR (600 MHz, DMSO-$d_6$): δ 8.92 (d, *J* = 7.4 Hz, 2H), 8.39−8.34 (m, 4H), 8.12 (d, *J* = 8.6 Hz, 4H), 7.91 (t, *J* = 7.5 Hz, 2H), 7.45 (t, *J* = 7.4 Hz, 1H). $^{13}$C NMR (151 MHz, DMSO-$d_6$): δ 147.0, 139.5, 139.4, 133.4, 127.9, 125.7, 124.9, 124.7, 118.2. IR (film, $cm^{-1}$): ν 3078 (C−H), 1358 (C−N), 853 (C−S). Mp: 170 °C (dec). MS (ESI). Calcd for $C_{20}H_{13}BiN_{10}O_4S_2$: *m/z* 765.0046 [(M + Cl)$^-$].

*[Bi($C_8H_7N_4S)_3$] **(3a)***. Following GP4, 1-(*p*-tolyl)-1*H*-tetrazole-5-thiol (75 mg, 0.39 mmol) and Bi(O$^t$Bu)$_3$ (55 mg, 0.13 mmol) were stirred in 5 mL of THF. The title compound was isolated as a bright-yellow solid (95 mg, 94%). $^1$H NMR (400 MHz, DMSO-$d_6$): δ 7.79 (d, *J* = 8.3 Hz, 6H), 7.29 (d, *J* = 8.1 Hz, 6H), 2.36 (s, 8H). $^{13}$C NMR (101 MHz, DMSO-$d_6$): δ 137.5, 134.4, 129.4, 124.1, 21.2. IR (film, $cm^{-1}$): ν 2858 (C−H), 1376 (C−N), 837 (C−S). Mp: 161 °C (dec). MS (ESI). Calcd for $C_{24}H_{21}BiN_{12}S_3$: *m/z* 817.0677 [(M + Cl)$^-$].

*[Bi($C_9H_{10}N_5S)_3$] **(3b)***. Following GP4, 1-(4-dimethylamino)phenyl)-1*H*-tetrazole-5-thiol (100 mg, 0.45 mmol) and Bi(O$^t$Bu)$_3$ (65 mg, 0.15 mmol) were stirred in 5 mL of THF. The title compound was isolated as a dark-orange solid (95 mg, 94%). $^1$H NMR (400 MHz, DMSO-$d_6$): δ 7.70−7.59 (m, 6H), 6.82−6.71 (m, 6H), 2.93 (s, 18H). $^{13}$C NMR (151 MHz, DMSO-$d_6$): δ 149.8, 125.0, 111.6, 40.1. IR (film, $cm^{-1}$): ν 2854 (C−H), 1357 (C−N), 814 (C−S). Mp: 150 °C (dec). MS (ESI). Calcd for $C_{27}H_{25}BiN_{15}S_3$: *m/z* 904.1466 [(M + Cl)$^-$].

*[Bi($C_{10}H_{11}N_4S)_3$] **(3c)***. Following GP4, 1-mesityl-1*H*-tetrazole-5-thiol (75 mg, 0.35 mmol) and Bi(O$^t$Bu)$_3$ (50 mg, 0.12 mmol) were stirred in 6 mL of THF. The title compound was isolated as a bright-yellow solid (80 mg, 85%). $^1$H NMR (400 MHz, DMSO-$d_6$): δ 7.06 (s, 6H), 2.31 (s, 9H), 1.85 (s, 18H). $^{13}$C NMR (101 MHz, DMSO-$d_6$): δ 135.3, 129.0, 20.7, 17.1. IR (film, $cm^{-1}$): ν 2917 (C−H), 1375 (C−N), 851 (C−S). Mp: 136−137 °C. MS (ESI). Calcd for $C_{30}H_{33}BiN_{12}S_3$: *m/z* 901.1693 [(M + Cl)$^-$].

*[Bi($C_7H_4ClN_4S)_3$] **(3d)***. Following GP4, 1-(4-chlorophenyl)-1*H*-tetrazole-5-thiol (75 mg, 0.34 mmol) and Bi(O$^t$Bu)$_3$ (50 mg, 0.12 mmol) were stirred in 6 mL of THF. The title compound was isolated as a bright-yellow solid (82 mg, 82%). $^1$H NMR (600 MHz, DMSO-$d_6$): δ 8.15−8.12 (m, 6H), 7.55−7.52 (m, 6H). $^{13}$C NMR (151 MHz, DMSO-$d_6$): δ 162.2, 136.4, 131.6, 128.8, 125.2, 40.5. IR (film, $cm^{-1}$): ν 2969 (C−H), 1374 (C−N), 839 (C−S). Mp: 147−149 °C. MS (ESI). Calcd for $C_{21}H_{12}BiCl_3N_{12}S_3$: *m/z* 876.9181 [(M + Cl)$^-$].

*[Bi($C_8H_7ON_4S)_3$] **(3e)***. Following GP4, 1-(4-methoxyphenyl)-1*H*-tetrazole-5-thiol (100 mg, 0.45 mmol) and Bi(O$^t$Bu)$_3$ (64 mg, 0.15 mmol) were stirred in 6 mL of THF. The crude mixture obtained was purified by recrystallization in ethyl acetate and hexane to yield the desired complex as a yellow solid (108 mg, 87%). $^1$H NMR (400 MHz, DMSO-$d_6$): δ 7.89−7.78 (m, 6H), 7.05−6.95 (m, 6H), 3.79 (s, 9H). $^{13}$C NMR (151 MHz, DMSO-$d_6$): δ 158.0, 130.1, 125.1, 113.5, 55.4. IR (film, $cm^{-1}$): ν 2934 (C−H), 1374 (C−N), 830 (C−S). Mp: 110−112 °C. MS (ESI). Calcd for $C_{24}H_{21}BiN_{12}O_3S_3$: *m/z* 865.0500 [(M + Cl)$^-$].

*[Bi($C_7H_4O_2N_5S)_3$] **(3f)***. Following GP4, 1-(4-nitrophenyl)-1*H*-tetrazole-5-thiol (100 mg, 0.45 mmol) and Bi(O$^t$Bu)$_3$ (64 mg, 0.15 mmol) were stirred in 6 mL of THF. The crude mixture obtained was purified by recrystallization in ethyl acetate and hexane to yield the desired complex as a yellow solid (116 mg, 90%). $^1$H NMR (400 MHz, DMSO-$d_6$): δ 8.49 (d, *J* = 8.8 Hz, 6H), 8.37 (d, *J* = 8.9 Hz, 6H). $^{13}$C NMR (151 MHz, DMSO-$d_6$): δ 124.3, 123.0. IR (film, $cm^{-1}$): ν 2924 (C−H), 1364 (C−N), 854 (C−S). Mp: 195−198 °C (dec). MS (ESI). Calcd for $C_{21}H_{12}BiN_{15}O_6S_3$: *m/z* 909.9750 [(M + Cl)$^-$].

*[Bi($C_{13}H_9N_4S)_3$] **(3g)***. Following GP4, triazolethiol **g** (380 mg, 1.5 mmol) and Bi(O$^t$Bu)$_3$ (215 mg, 0.5 mmol) were stirred in 10 mL of THF. The title complex was isolated as a yellow solid (280 g, 58%). $^1$H NMR (400 MHz, DMSO-$d_6$): δ 8.53 (d, *J* = 5.2 Hz, 2H), 7.51 (s, 3H), 7.37 (d, *J* = 6.2 Hz, 2H), 7.21 (d, *J* = 5.1 Hz, 2H). $^{13}$C NMR (151 MHz, DMSO-$d_6$): δ 150.0, 134.7, 133.6, 129.4, 128.58, 121.6. IR (film, $cm^{-1}$): ν 1495 (C−N), 1298 (C−C−N), 1285 (C−N), 830 (C−S). Mp: 197 °C (dec). MS (ESI). Calcd for $C_{29}H_{36}BiCl_2N_8O_6S_3$: *m/z* 935.4728 ([$L_2$Bi·$CH_2Cl_2$·6$H_2O$]$^+$).

*[Bi($C_{14}H_{11}N_4S)_3$](**3h**)*. Following GP4, triazolethiol **h** (400 mg, 1.5 mmol) and Bi(O$^t$Bu)$_3$ (215 mg, 0.5 mmol) were stirred in 10 mL of THF. The title complex was isolated as a yellow solid (347 mg, 69%). $^1$H NMR (400 MHz, DMSO-$d_6$): δ 8.52 (d, *J* = 6.2 Hz, 2H), 8.24 (d, *J* = 7.3 Hz, 4H), 7.54 (t, *J* = 7.6 Hz, 4H), 7.35−7.28 (m, 1H), 7.28−7.18 (m, 2H), 7.03 (d, *J* = 8.9 Hz, 1H). $^{13}$C NMR (151 MHz, DMSO-$d_6$): δ 149.9, 138.8, 133.9, 129.8, 128.3, 121.4, 20.8. IR (film, $cm^{-1}$): ν 1423 (C−N), 1259 (C−C−N), 821 (C−S). Mp: 190 °C (dec). MS (ESI). Calcd for $C_{42}H_{33}BiN_{12}S_3$: *m/z* 1033.9881 [(M − H)$^-$].

*[Bi($C_{14}H_{11}N_4OS)_3$] **(3i)***. Following GP4, triazolethiol **i** (425 mg, 1.5 mmol) and Bi(O$^t$Bu)$_3$ (215 mg, 0.5 mmol) were stirred in 10 mL of THF. The title complex was isolated as an orange solid (280 mg, 53%). $^1$H NMR (400 MHz, DMSO-$d_6$): δ 8.62−8.37 (m, 2H), 7.26 (dd, *J* = 20.5 and 6.7 Hz, 4H), 7.04 (d, *J* = 8.4 Hz, 2H), 3.81 (s, 3H). $^{13}$C NMR (151 MHz, DMSO-$d_6$): δ 159.6, 129.8, 121.6, 114.6, 55.4. IR (film, $cm^{-1}$): ν 1251 (C−C−N), 826 (C−S). Mp: 191 °C (dec). MS (ESI). Calcd for $C_{30}H_{42}BiN_8O_{10}S_2$: *m/z* 947.4937 ([$L_2$Bi·2$CH_3OH$·6$H_2O$]$^+$).

*[Bi($C_{13}H_8N_4ClS)_3$] **(3j)***. Following GP4, triazolethiol **j** (408 mg, 1.5 mmol) and Bi(O$^t$Bu)$_3$ (215 mg, 0.5 mmol) were stirred in 10 mL of THF. The title complex was isolated as a bright-orange solid (303 mg, 57%). $^1$H NMR (400 MHz, DMSO-$d_6$): δ 8.53 (d, *J* = 5.1 Hz, 2H), 7.56 (d, *J* = 8.3 Hz, 2H), 7.39 (d, *J* = 8.2 Hz, 2H), 7.21 (d, *J* = 5.1 Hz, 2H). $^{13}$C NMR (151 MHz, DMSO-$d_6$): δ 113.0, 100.4, 96.07, 93.4, 92.3, 91.2, 84.4. IR (film, $cm^{-1}$): ν 1492 (C−H), 1424 (C−N), 1091 (C−C−N), 826 (C−S). Mp: 192 °C (dec). MS (ESI). Calcd for $C_{28}H_{20}BiCl_6N_8S_2$: *m/z* 951.4693 ([$L_2$Bi·2$CH_2Cl_2$]$^+$).

*[Bi($C_{13}H_8N_4FS)_3$] **(3k)***. Following GP4, triazolethiol **k** (432 mg, 1.5 mmol) and Bi(O$^t$Bu)$_3$ (215 mg, 0.5 mmol) were stirred in 10 mL of THF. The title complex was isolated as a yellow solid (336 mg, 66%). $^1$H NMR (400 MHz, DMSO-$d_6$): δ 8.62−8.43 (m, 2H), 7.30−7.10 (m, 5H). $^{13}$C NMR (151 MHz, DMSO-$d_6$): δ 162.9, 161.2, 150.0, 148.5, 133.6, 131.1, 131.0, 130.9, 121.6, 116.4, 116.3. IR (film, $cm^{-1}$): ν 1602 (C−C), 1427 (C−N), 1216 (C−C−N), 839 (C−S), 827 (C−S). Mp: 237 °C (dec). MS (ESI). Calcd for $C_{39}H_{24}BiF_3N_{12}S_3$: *m/z* 1087.2122 [(M + MeOH)$^-$].

*[Bi($C_{15}H_{13}N_4S)_3$] **(3l)***. Following GP4, triazolethiol **l** (423 mg, 1.5 mmol) and Bi(O$^t$Bu)$_3$ (215 mg, 0.5 mmol) were stirred in 10 mL of THF. The title complex was isolated as a yellow solid (463 mg, 88%). $^1$H NMR (400 MHz, DMSO-$d_6$): δ 8.54 (d, *J* = 5.2 Hz, 2H), 7.49−6.90 (m, 5H), 2.35 (s, 3H), 1.97 (s, 3H). $^{13}$C NMR (151 MHz, DMSO-$d_6$): δ 150.2, 139.6, 135.5, 133.5, 131.7, 131.2, 128.8, 127.9, 120.6, 20.8, 17.3. IR (film, $cm^{-1}$): ν 1298 (C−N), 825 (C−S). Mp: 171 °C (dec). MS (ESI). Calcd for $C_{45}H_{39}BiN_{12}S_3$: *m/z* 1129.2619 [(M + DMSO)$^-$].


https://dx.doi.org/10.1021/acs.inorgchem.9b03550
Inorg. Chem. XXXX, XXX, XXX−XXX

## ■ ASSOCIATED CONTENT

### Supporting Information

The Supporting Information is available free of charge at https://pubs.acs.org/doi/10.1021/acs.inorgchem.9b03550.

Experimental data (preparation of tetrazole and triazole thiolates), crystallography details, and NMR ($^{1}$H and $^{13}$C) spectra (PDF)

### Accession Codes

CCDC 1968616−1968625 contain the supplementary crystallographic data for this paper. These data can be obtained free of charge via www.ccdc.cam.ac.uk/data_request/cif, or by emailing data_request@ccdc.cam.ac.uk, or by contacting The Cambridge Crystallographic Data Centre, 12 Union Road, Cambridge CB2 1EZ, UK; fax: +44 1223 336033.

## ■ AUTHOR INFORMATION


### Corresponding Author

**Philip C. Andrews** − *Monash University School of Chemistry, Clayton, Victoria 3800, Australia;* orcid.org/0000-0002-3971-7311; Email: phil.andrews@monash.edu

### Authors

**Liam J. Stephens** − *Monash University School of Chemistry, Clayton, Victoria 3800, Australia*

**Sarmishta Munuganti** − *Monash University School of Chemistry, Clayton, Victoria 3800, Australia*

**Rebekah N. Duffin** − *Monash University School of Chemistry, Clayton, Victoria 3800, Australia*

**Melissa V. Werrett** − *Monash University School of Chemistry, Clayton, Victoria 3800, Australia;* orcid.org/0000-0001-6811-4504

Complete contact information is available at: https://pubs.acs.org/10.1021/acs.inorgchem.9b03550


### Author Contributions

†The manuscript was written through contributions of all authors. All authors have given approval to the final version of the manuscript. These authors contributed equally.

### Notes

The authors declare no competing financial interest.

## ■ ACKNOWLEDGMENTS

The authors acknowledge the use of facilities within the Monash X-ray Platform and the assistance of Dr. Craig Forsyth for assistance with single-crystal X-ray crystallography. The authors also acknowledge the use of facilities within the Monash Centre for Electron Microscopy and the Ramaciotti Centre for Cryo Electron Microscopy and are thankful to the assistance provided by Dr. Xiya Fang and Dr. Simon Crawford, respectively. The authors also acknowledge the use of facilities within the Monash Analytical Platform.

## ■ REFERENCES


(1) O'Neill, J. *Tackling Drug-Resistant Infections Globally: Final Report and Recommendations*, 2016.

(2) McCarthy, M. Woman Dies after Infection with Bacteria Resistant to All Antibiotics Available in US. *BMJ.* **2017**, *356*, j254.

(3) Chen, L.; Todd, R.; Kiehlbauch, J.; Walters, M.; Kallen, A. Notes from the Field: Pan-Resistant New Delhi Metallo-Beta-Lactamase-Producing Klebsiella Pneumoniae — Washoe County, Nevada, 2016. *Morb. Mortal. Wkly. Rep.* **2017**, *66*, 33.

(4) Ventola, C. L. The Antibiotic Resistance Crisis: Part 1: Causes and Threats. *Pharm. Ther.* **2015**, *40*, 277−283.

(5) Hobman, J. L.; Crossman, L. C. Bacterial Antimicrobial Metal Ion Resistance. *J. Med. Microbiol.* **2015**, *64*, 471−497.

(6) Gunawan, C.; Marquis, C. P.; Amal, R.; Sotiriou, G. A.; Rice, S. A.; Harry, E. J. Widespread and Indiscriminate Nanosilver Use: Genuine Potential for Microbial Resistance. *ACS Nano* **2017**, *11*, 3438−3445.

(7) Maillard, J.-Y.; Hartemann, P. Silver as an Antimicrobial: Facts and Gaps in Knowledge. *Crit. Rev. Microbiol.* **2013**, *39*, 373−383.

(8) Mohan, R. Green Bismuth. *Nat. Chem.* **2010**, *2*, 336.

(9) Sadler, P. J.; Li, H.; Sun, H. Coordination Chemistry of Metals in Medicine: Target Sites for Bismuth. *Coord. Chem. Rev.* **1999**, *185−186*, 689−709.

(10) Li, H.; Sun, H. Recent Advances in Bioinorganic Chemistry of Bismuth. *Curr. Opin. Chem. Biol.* **2012**, *16*, 74−83.

(11) Wang, R.; Lai, T.-P.; Gao, P.; Zhang, H.; Ho, P.-L.; Woo, P. C.-Y.; Ma, G.; Kao, R. Y.-T.; Li, H.; Sun, H. Bismuth Antimicrobial Drugs Serve as Broad-Spectrum Metallo-$\beta$-Lactamase Inhibitors. *Nat. Commun.* **2018**, *9*, 439.

(12) Luqman, A.; Blair, V. L.; Brammananth, R.; Crellin, P. K.; Coppel, R. L.; Andrews, P. C. The Importance of Heterolepticity in Improving the Antibacterial Activity of Bismuth(III) Thiolates. *Eur. J. Inorg. Chem.* **2016**, *2016*, 2738−2749.

(13) Luqman, A.; Blair, V. L.; Brammananth, R.; Crellin, P. K.; Coppel, R. L.; Andrews, P. C. Homo- and Heteroleptic Bismuth (III/V) Thiolates from N- Heterocyclic Thiones: Synthesis, Structure and Anti-Microbial Activity. *Chem. - Eur. J.* **2014**, *20*, 14362−14377.

(14) Luqman, A.; Blair, V. L.; Brammananth, R.; Crellin, P. K.; Coppel, R. L.; Kedzierski, L.; Andrews, P. C. Homoleptic and Heteroleptic Bismuth(III) Thiazole-Thiolates and the Influence of Ring Substitution on Their Antibacterial and Antileishmanial Activity. *Eur. J. Inorg. Chem.* **2015**, *2015*, 725−733.

(15) Pathak, A.; Blair, V. L.; Ferrero, R. L.; Kedzierski, L.; Andrews, P. C. Structural Influences on the Activity of Bismuth(III) Indole-Carboxylato Complexes towards Helicobacter Pylori and Leishmania. *J. Inorg. Biochem.* **2017**, *177*, 266−275.

(16) Werrett, M. V.; Herdman, M. E.; Brammananth, R.; Garusinghe, U.; Batchelor, W.; Crellin, P. K.; Coppel, R. L.; Andrews, P. C. Bismuth Phosphinates in Bi-Nanocellulose Composites and Their Efficacy towards Multi-Drug Resistant Bacteria. *Chem. - Eur. J.* **2018**, *24*, 12938−12949.

(17) Egorova, K. S.; Ananikov, V. P. Toxicity of Metal Compounds: Knowledge and Myths. *Organometallics* **2017**, *36*, 4071−4090.

(18) Mendelowitz, P. C.; Hoffman, R. S.; Weber, S. Bismuht Absorption and Myoclonic Encephalopathy during Bismuth Subsalicylate Therapy. *Ann. Intern. Med.* **1990**, *112*, 140−141.

(19) Borbinha, C.; Serrazina, F.; Salavisa, M.; Viana-Baptista, M. Bismuth Encephalopathy- A Rare Complication of Long-Standing Use of Bismuth Subsalicylate. *BMC Neurol.* **2019**, *19*, 212.

(20) Hogan, D. B.; Harbidge, C.; Duncan, A. Bismuth Toxicity Presenting as Declining Mobility and Falls. *Can. Geriatr. J.* **2018**, *21*, 307−309.

(21) Hutson, J. C. Effects of Bismuth Citrate on the Viability and Function of Leydig Cells and Testicular Macrophages. *J. Appl. Toxicol.* **2005**, *25*, 234−238.

(22) Zhou, C. H.; Wang, Y. Recent Researches in Triazole Compounds as Medicinal Drugs. *Curr. Med. Chem.* **2012**, *19*, 239−280.

(23) Mittal, R.; Awasthi, S. K. Recent Advances in the Synthesis of 5-Substituted 1H-Tetrazoles: A Complete Survey (2013−2018). *Synthesis* **2019**, *51*, 3765−3783.

(24) Stavila, V.; Whitmire, K. H.; Rusakova, I. Synthesis of $Bi_2S_3$ Nanostructures from Bismuth(III) Thiourea and Thiosemicarbazide Complexes. *Chem. Mater.* **2009**, *21*, 5456−5465.

(25) Farrugia, L. J.; Lawlor, F. J.; Norman, N. C. Co-ordination Complexes of the Bismuth(III) Thiolate Bi $(SC_6F_5)_3$. *J. Chem. Soc., Dalton Trans.* **1995**, 1163−1171.




https://dx.doi.org/10.1021/acs.inorgchem.9b03550
*Inorg. Chem.* XXXX, XXX, XXX−XXX

(26) Domenico, P.; Baldassarri, L.; Schoch, P. E.; Kaehler, K.; Sasatsu, M.; Cunha, B. A. Activities of Bismuth Thiols against Staphylococci and Staphylococcal Biofilms. *Antimicrob. Agents Chemother.* **2001**, *45*, 1417−1421.
(27) Wu, C.; Domenico, P.; Hassett, D. J.; Beveridge, T. J.; Hauser, A. R.; Kazzaz, J. A. Subinhibitory Bismuth-Thiols Reduce Virulence of Pseudomonas Aeruginosa. *Am. J. Respir. Cell Mol. Biol.* **2002**, *26*, 731−738.
(28) Luqman, A.; Blair, V. L.; Brammananth, R.; Crellin, P. K.; Coppel, R. L.; Andrews, P. C. Powerful Antibacterial Activity of Phenyl-Thiolatobismuth(III) Complexes Derived from Oxadiazole-thiones. *Eur. J. Inorg. Chem.* **2015**, *2015*, 4935−4945.
(29) Lieber, E.; Ramachandran, J. Isomeric 5-(substituted) amino-thiatriazole and 1-substituted-tetrazolinethiones'. *Can. J. Chem.* **1959**, *37*, 101.
(30) Megally Abdo, N. Y.; Kamel, M. M. Synthesis and Anticancer Evaluation of 1,3,4-Oxadiazoles, 1,3,4-Thiadiazoles, 1,2,4-Triazoles and Mannich Bases. *Chem. Pharm. Bull.* **2015**, *63*, 369−376.
(31) Luqman, A.; Blair, V. L.; Bond, A. M.; Andrews, P. C. Formation of Bismuth(V) Thiolates: Protolysis and Oxidation of Triphenylbismuth(III) with Heterocyclic Thiols. *Angew. Chem., Int. Ed.* **2013**, *52*, 7247−7251.
(32) Burford, N.; Eelman, M. D.; Mahony, D. E.; Morash, M. Definitive Identification of Cysteine and Glutathione Complexes of Bismuth by Mass Spectrometry: Assessing the Biochemical Fate of Bismuth Pharmaceutical Agents. *Chem. Commun.* **2003**, 146−147.
(33) Andrews, P. C.; Busse, M.; Deacon, G. B.; Ferrero, R. L.; Junk, P. C.; Huynh, K. K.; Kumar, I.; Maclellan, J. G. Structural and Solution Studies of Phenylbismuth(III) Sulfonate Complexes and Their Activity against Helicobacter Pylori. *Dalton Trans.* **2010**, *39*, 9633−9641.
(34) Domenico, P.; Salo, R. J.; Novick, S. G.; Schoch, P. E.; Van Horn, K.; Cunha, B. A. Enhancement of Bismuth Antibacterial Activity with Lipophilic Thiol Chelators. *Antimicrob. Agents Chemother.* **1997**, *41*, 1697−1703.
(35) Kotani, T.; Nagai, D.; Asahi, K.; Suzuki, H.; Yamao, F.; Kataoka, N.; Yagura, T. Antibacterial Properties of Some Cyclic Organobismuth (III) Compounds. *Antimicrob. Agents Chemother.* **2005**, *49*, 2729−2734.
(36) Farkas, A.; Maróti, G.; Kereszt, A.; Kondorosi, É. Comparative Analysis of the Bacterial Membrane Disruption Effect of Two Natural Plant Antimicrobial Peptides. *Front. Microbiol.* **2017**, *8*, 1−12.
(37) Payne, D. J.; Gwynn, M. N.; Holmes, D. J.; Pompliano, D. L. Drugs for Bad Bugs: Confronting the Challenges of Antibacterial Discovery. *Nat. Rev. Drug Discovery* **2007**, *6*, 29−40.
(38) Pritchett, J. C.; Naesens, L.; Montoya, J. *Treating HHV-6 Infections: The Laboratory Efficacy and Clinical Use of Anti-HHV-6 Agents*; Elsevier BV, 2014.
(39) Rodríguez, A.; Villegas, E.; Montoya-Rosales, A.; Rivas-Santiago, B.; Corzo, G. Characterization of Antibacterial and Hemolytic Activity of Synthetic Pandinin 2 Variants and Their Inhibition against Mycobacterium Tuberculosis. *PLoS One* **2014**, *9*, e101742.
(40) Ciornei, C. D.; Sigurdardóttir, T.; Schmidtchen, A.; Bodelsson, M. Antimicrobial and Chemoattractant Activity, Lipopolysaccharide Neutralization, Cytotoxicity, and Inhibition by Serum of Analogs of Human Cathelicidin LL-37. *Antimicrob. Agents Chemother.* **2005**, *49*, 2845−2850.
(41) Mansfeld, D., Technische Universität Chemnitz, Chemnitz, Germany, 2009.


https://dx.doi.org/10.1021/acs.inorgchem.9b03550
*Inorg. Chem.* XXXX, XXX, XXX−XXX